

UC Berkeley

Sustainability, Whole Building Energy and Other Topics

Title

Transformation Towards a Carbon-Neutral Residential Community with Hydrogen Economy and Advanced Energy Management Strategies

Permalink

<https://escholarship.org/uc/item/61g3g267>

Authors

He, Yingdong
Zhou, Yuekuan
Yuan, Jing
[et al.](#)

Publication Date

2021-10-09

DOI

10.1016/j.enconman.2021.114834

Copyright Information

This work is made available under the terms of a Creative Commons Attribution-NonCommercial-ShareAlike License, available at <https://creativecommons.org/licenses/by-nc-sa/4.0/>

Peer reviewed

Transformation towards a carbon-neutral residential community with hydrogen economy and advanced energy management strategies

Yingdong He^{1, 3}, Yuekuan Zhou^{2, *}, Jing Yuan¹, Zhengxuan Liu³, Zhe Wang⁴, Guoqiang Zhang³

¹*Center for the Built Environment, University of California, Berkeley, Berkeley CA, U.S.A.*

²*Department of Mechanical and Aerospace Engineering, The Hong Kong University of Science and Technology, Clear Water Bay, Hong Kong SAR, China*

³*College of Civil Engineering, Hunan University, Changsha, Hunan, China*

⁴*Building Technology and Urban Systems Division, Lawrence Berkeley National Laboratory, Berkeley, CA, U.S.A.*

Abstract: Cleaner power production, distributed renewable generation, building-vehicle integration, hydrogen storage and associated infrastructures are promising for transformation towards a carbon-neutral community, whereas the academia provides limited information through integrated solutions, like intermittent renewable integration, hydrogen sharing network, smart operation on electrolyzer and fuel cell, seasonal hydrogen storage and advanced heat recovery. This study proposes a hybrid electricity-hydrogen sharing system in California, United States, with synergistic electric, thermal and hydrogen interactions, including low-rise houses, rooftop photovoltaic panels, hydrogen vehicles, a hydrogen station, micro and utility power grid and hydrogen pipelines. Advanced energy management strategies were proposed to enhance energy flexibility and grid stability. Besides, simulation-based optimizations on smart power flows of vehicle-to-grid interaction and electrolyzer are conducted for further seasonal grid stability and annual cost saving. The obtained results indicate that, the green renewable-to-hydrogen can effectively reduce reliance on pipelines delivered hydrogen, and the hydrogen station is effective to address security concerns of high-pressure hydrogen and improve participators' acceptance. Microgrid peer-to-peer sharing can improve hydrogen system efficiency under idling modes. Furthermore, the integrated system can reduce the annual net hydrogen consumption in transportation from 127.0 to 1.2 kg/vehicle. The smart operation (minimum input power of electrolyzer and fuel cell at 65 and 80 kW) can reduce the maximum mean hourly grid power to 78.2 kW by 24.2% and the annual energy cost to 1228.5 \$/household by 38.9%. The proposed district hydrogen-based community framework can provide cutting-edge techno-economic guidelines for carbon-neutral transition with district peer-to-peer energy sharing, zero-energy buildings, hydrogen-based transportations together with smart strategies for high energy flexibility.

Keywords: Solar Energy; Distributed Renewable Energy Sharing; Flexible Energy Management Strategy; Hydrogen Energy Storage and Economy; Distributed Hydrogen Infrastructure.

Corresponding author: Tel.: (+852) 2766 4560

Email: yuekuan.zhou@connect.polyu.hk

yuekuan.zhou@outlook.com (Zhou Y.)

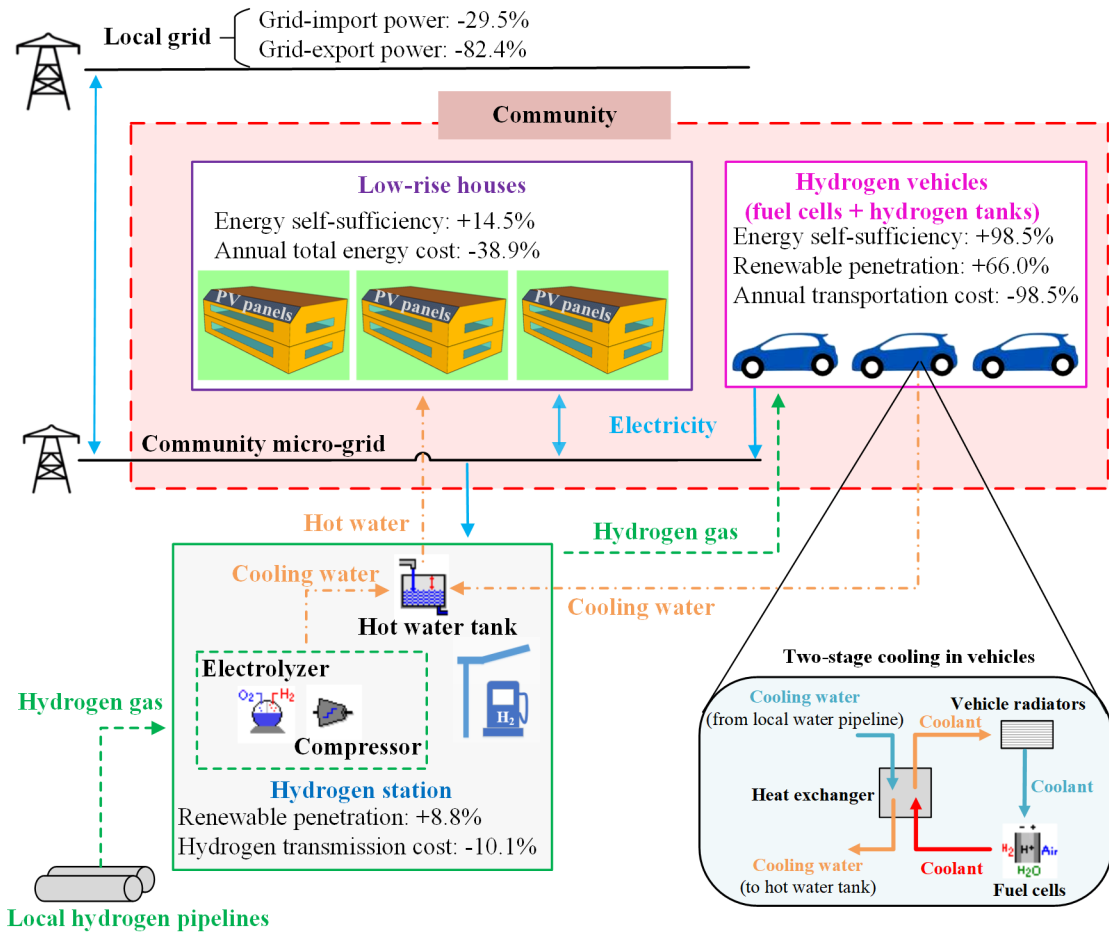
Energy Conversion and Management, October 2021, Volume 249

1

<https://doi.org/10.1016/j.enconman.2021.114834>

<https://escholarship.org/uc/item/61g3g267>

Graphical abstract:



1 Introduction

Building and transportation sectors are the major energy consumers of the modern world. For example, in Europe, the building and transportation sectors consume around 60% of the total energy [1]. In the United States of America (U.S.A.), the building and transportation sectors represented 28% and 37% of the total end-use energy in 2019, respectively, reaching up to 21.3 and 28.2 quadrillion Btu [2]. On the one hand, a huge amount of energy consumed by buildings and transportation is necessary for providing thermally comfortable indoor environments (especially, space heating in winter [3] and space cooling in summer [4]) and convenience for daily activities (such as working, shopping, traveling, and so on) [5]. On the other hand, the huge amount of energy consumed by buildings and transportation causes irreversible damages to the natural environment and imposes a heavy burden on current energy networks, which require the capacity expansion of current energy infrastructures, such as electric power grid and vehicle refueling stations.

A possible solution for covering district energy demands with reduced reliance on traditional fossil fuels is to deploy renewables for cleaner power production. For example, the wide deployment of distributed building integrated renewable systems, such as photovoltaic (PV) and wind energy, directly reduces the amount of electricity imported from the power grid. In terms of transportation, using renewable electricity or renewable-produced fuels for daily travel can reduce the dependence on fossil fuels. The replacement of non-renewables such as fossil fuels by renewables in buildings and vehicles will significantly reduce environmental pollution for climate change mitigation without lowering

people's living standards or increasing the burden of current energy infrastructure. Besides, when being integrated with multiple energy storages such as electrochemical, thermal, and hydrogen (H₂) storages, renewables can further improve regional energy flexibility and grid power stability. For example, shifting renewables from the grid to the H₂ production for daily and seasonal energy storages and transportation energy use, helps to reduce the grid instability due to the intermittent electricity production of renewable systems (wind turbines, PV, and more) [6], which is an attractive and practical solution for mismatched energy generation and demand profiles [7]. Furthermore, for energy flexibility enhancement, micro-grids, systematically connecting district buildings, vehicles, and other energy infrastructures, are full of prospects to practically penetrate renewables in buildings and vehicles. Compared to a purely grid-connected energy network with buildings, the integration of buildings and vehicles actualizes energy complementarity for different energy networks, such as the power grid and H₂ pipeline-based grid, which shows promising benefits in terms of renewable penetration, energy self-sufficiency [8], grid stability, and energy cost reduction [9].

In order to form integrated energy systems, the deployment of building-vehicle system with renewable energy is critical for the realization of zero-energy buildings and transportations. Recently, due to the fast expansion of H₂ energy technologies and market [10] as well as the clean byproduct (water), fuel-cell-driven hydrogen vehicles (HVs) are gaining increased popularity and regarded as one of the most promising techniques for carbon-neutral community transition. A series of HVs using hydrogen gas (H₂ gas) as fuels have been promoted, such as Toyota's Mirai cars [11] and Honda's CLARITY cars [12], to replace the conventional vehicles (non-renewable fossil fuels, such as diesel and gasoline vehicles). Moreover, compared to electrical vehicles (EVs), HVs show a relatively higher cruise distance, i.e., a cruise distance over 500 km and 200-300 km after being fully charged for HVs and EVs, respectively [13]. The longer cruise distance of HVs makes them more attractive and socially acceptable than EVs in terms of cruise anxiety. Besides, the H₂-electricity conversion procedure in the proton exchange membrane fuel cells (PEMFCs) of HVs can be incorporated in the regional network for actualizing H₂-electricity interactions for the coverage of building energy demands. As a result, HVs can play a role as an energy carrier rather than only an energy consumer in regional energy systems. Furthermore, integrating buildings and HVs achieves the energy complementarity of regional electricity and H₂ networks, which makes it possible and attractive to establish H₂-electricity-supported building-vehicle systems with high renewable penetration, grid stability, and low energy cost.

1. Relevant research progress

In recent years, some researchers have started to explore the benefits of integrating buildings and HVs in regional energy networks. When integrating with one or several buildings, renewables can be converted into H₂, and then charged to HV tanks to meet transportation energy demands. The renewable-H₂ conversion process reduces renewable congestion in the power grid and decreases fossil fuel consumption for transportations (HVs instead of gasoline vehicles). HVs can also be charged in H₂ stations, and then the stored H₂ in vehicle tanks can be discharged to power buildings during the energy shortage period (i.e., V2B interaction). In this sense, the H₂-electricity process reduces the grid congestion burden and enhances the energy storage capacity for buildings with the expansion of energy boundary including the H₂ station. Mehrjerdi et al. [14] formulated a building-vehicle energy system integrating a house, PV panels, wind turbines, an electrolyzer, and HVs. The system performance was investigated in two cases: one was connected to the power grid, and another one was not. They found that, compared to the traditional house with gasoline vehicles, the building-vehicle energy system supported by renewables reduced the annual CO₂ emission by 12.5%. Robledo et al. [15] carried out a two-week experimental investigation on the feasibility of energy interaction between a house and a HV in Netherlands. The HV was charged at a nearby H₂ fueling station and discharged H₂ for powering the house. The results indicated that the V2B interaction covered 71% of the annual electricity demand of the house, providing a good reference for enhancing the building energy independence and grid stability. Farahani et al. [16]

designed an energy network integrating an office building, wind turbines, PV systems, EVs and HVs as energy carriers. The wind turbines were used to produce H₂, which was later discharged by PEMFCs in vehicles for daily transportation and powering the office building. They found that such an energy network was 100% self-sufficient by renewables, with the stored energy by vehicles covering up to 30% of the total energy demand. Cao and Alanne [17] built a model of a residential building integrated with an onsite renewable system and a HV. They found that deploying a domestic electrolyzer can transfer the surplus renewable energy from the building to the HV, which finally achieved the net-zero energy use for both the building and vehicle.

In addition to directly powering one or several buildings, HVs can also power the local electric grid (i.e., V2G interaction) to improve the grid reliability for demand coverage with energy flexibility, in response to intermittent and fluctuated renewable generations. Felgenhauer et al. [18] did a case study of a community with 8000-residential buildings, renewable systems and HVs, where the electricity driven H₂ was to cover daily transportation demand. They pointed out that more than 80% of the H₂ was produced using the renewable electricity, rather than the grid-imported electricity, achieving a high renewable penetration rate into transportation energy system. Sahu et al. [19] investigated the V2G interaction by 500 HVs for the power coverage of energy shortage of 1000 houses. The results indicated that the V2G integration by HVs covered 80% of the energy demands, which significantly reduced the local grid's burden. Alavi et al. [20] established a community model that integrated buildings, PV panels, wind turbines, and HVs. The renewable electricity generated by PV panels and wind turbines was used to cover building demands and produce H₂ for daily transportation. The V2G interaction was also used by discharging the H₂ in HV tanks to power the community micro-grid. The results indicated that the community micro-grid's maximum power was reduced by nearly 50% after the V2G interaction was applied. Oldenbroek et al. [21] analyzed the benefits of a smart city consisting of distributed PV and wind turbine systems, houses, H₂ stations, and HVs with V2G interaction. Such a smart city actualizes a favorable cost of transportation by HVs at 0.02 euro/km. From the perspective of national grid stability, Oldenbroek et al. [22] analyzed the feasibility of incorporating HVs as the expanded energy storage for storing surplus renewables and covering the energy shortage of Germany's national grid. They found that the incorporated HVs covered up to 63 GW of the grid energy shortage of the nation-wide electricity, heating, and transportation systems.

1.2 Prospects of hydrogen energy in United States and California

Considering the considerable advantages of H₂ energy in terms of regional energy flexibility, cleaner power production, grid stability, and environmental pollution reduction, in 2020, the U.S.A. formulated an ambitious blueprint for national H₂ energy application and H₂ economy, which is called the Road Map to a Hydrogen Economy [23]. Although the H₂ energy was negligible in the end-use energy demand of the U.S.A. in 2015 [23], the final goal of this blueprint is to elevate the H₂ energy proportion to 14% of the annual national end-use energy by 2050, which includes 4, 8, 27 million tons of H₂ for grid balance, buildings, and transportation, respectively. Moreover, as shown in Fig. 1, by 2030, it is expected to sell more than 1 million HVs and build more than 5000 H₂ stations in the U.S.A., providing half a million new jobs related to H₂ energy. This blueprint will stimulate the rapid development of H₂ energy industries and H₂-based energy networks of the U.S.A. in the coming years.






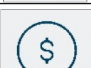

		Today	2022	2025	2030
		Immediate next steps	Early scale-up	Diversification	Broad rollout
H ₂ demand, metric tons		11 m	12 m	13 m	17 m
FCEV scales		2,500	30,000	150,000	1,200,000
Material-handling FCEVs		25,000	50,000	125,000	300,000
Fuelling stations ¹		63	165 ²	10,00 ²	43,00 ³
Material-handling fuelling stations ⁴		120	300	600	1,500
Annual investment			\$ 1 bn	\$ 2 bn	\$ 8 bn
New jobs ⁵			+50,000	+100,000	+500,000

Fig. 1. The medium-term goal of the hydrogen economy of the U.S.A. by 2030 (originally from the reference [23]).

(1. Includes both fueling stations in operation and in development

2. Station of 500 kg/day; does not include material-handling fueling stations

3. Stations of 1000 kg/day; does not include material-handling fueling stations

4. Data from Plug Power

5. Include direct, indirect and resulting jobs, building on an estimated 200,000 jobs in the sector today

FCEVs means the fuel cell electric vehicles, which are hydrogen vehicles.)

California, which is located at the west coast of the U.S.A. and featured with abundant solar radiation, has proposed the Renewables Portfolio Standard to mandatorily require California energy-supply companies and organizations to expand their renewable energy resources (solar, wind, geothermal, biomass, and hydroelectric) for actualizing a goal of 60% renewable in the total regional energy consumption by 2030 [24]. To date, in California, the buildings (residential and commercial) and transportation consume more than 75% of the total regional energy (Fig. 2(a)) [25]. Supposed that renewables can cover these two sectors, the renewable ratio of the total regional energy of California can be significantly increased from the current level (around 35%, see Fig. 2(b)) to the expected level (60%) by 2030 [24]. The annual renewable power energy of California in 2019 is 105559 GWh [24]. The annual renewable production of U.S.A. in 2019 is 3378230 GWh [26]. The ratio of renewable energy of California to U.S.A. renewable energy production is 3.1%.

To actualize the high renewable penetration into the total regional energy consumption, California becomes a forerunner of H₂ energy development and application in the U.S.A., under a fast expansion of H₂ infrastructure for cleaner energy use in transportation. Currently, California has built 42 H₂ stations for charging HVs, and 15 more H₂ stations are under construction [27]. By 2030, California is expected to have 1000 H₂ station and one million HVs, which saves 2.63 million m³ of gasoline used by conventional vehicle fleets [28]. Furthermore, the cost of each HV is usually \$50000-\$70000, but multiple subsidies are offered to the buyers for promoting zero-emission vehicles. For example, the Toyota Mirai HVs are about \$50000 per vehicle, but the Toyota company offers an up to \$15000 subsidy for customers after purchasing [29]. Also, California offers an additional \$4500 subsidy for the buyers [30]. As a result, the cost of HVs can be lowered to around \$35000, which can be afforded by medium class families.

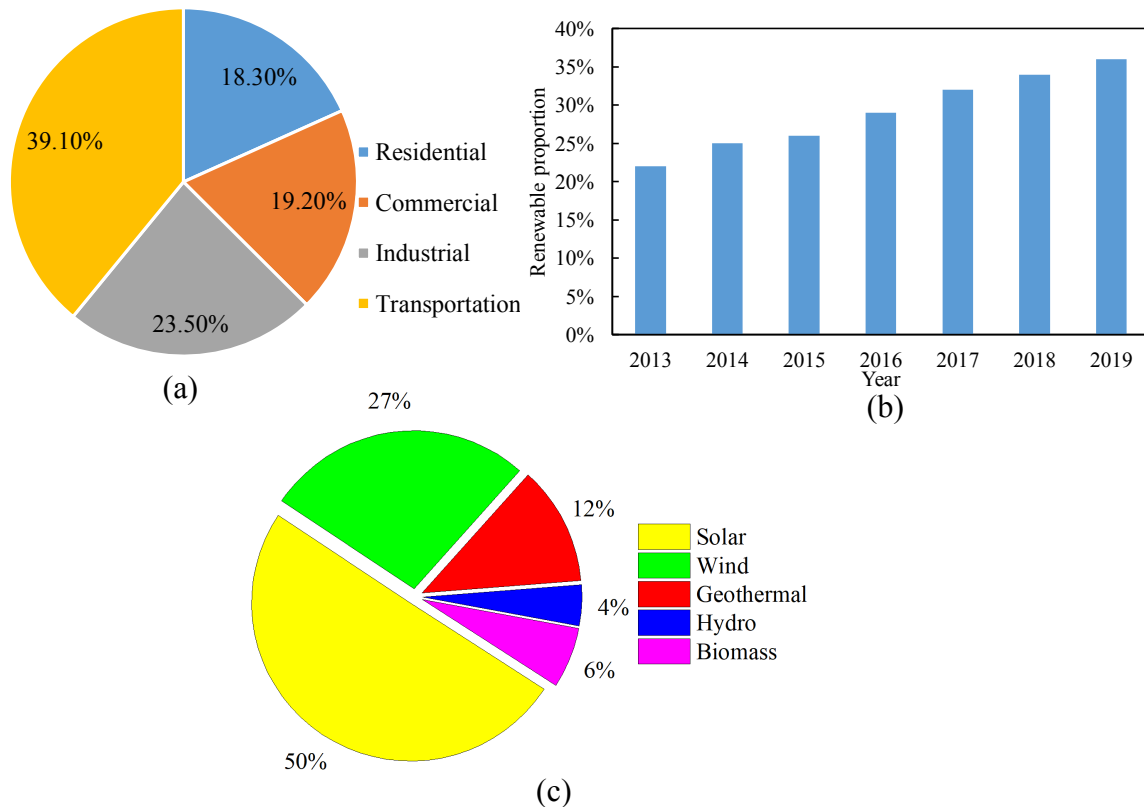


Fig. 2. (a) Energy use across sectors of California in 2018 (originally from the reference [25]), (b) renewable ratios in total energy consumption of California from 2013 to 2019 (originally from the reference [24]), and (c) renewable ratios in total renewable energy of California in 2019 (originally from the reference [24]).

Nonetheless, to date, in California, the main function of local H₂ stations is designed only to supply H₂ to HVs for covering transportation energy demands, without establishing diversified energy interactions with local buildings and other energy infrastructure. Such a limited role of H₂ stations in the current local energy network will indeed restrain and block the development and application of H₂ facilities, whereas the participation of H₂ stations in the local energy network for energy sharing is full of promising prospects. Furthermore, the energy performance of buildings and HVs is better to be investigated with consideration into the local energy policy and available H₂ infrastructure. California provides many chances for the configuration of energy interactions between local electricity and H₂ networks to enhance regional renewable penetration, energy flexibility, grid stability, energy efficiency, and cost-saving. However, few studies explored the availability and practicability of H₂-based interactive energy networks, consisting of renewable systems, buildings, local electric grid, HVs, and H₂ stations in California, to realize the regional carbon-neutrality.

1.3 Scientific gaps

Despite of significant advantages of the integration of buildings, vehicles, and H₂ systems, the current academia shows little progress towards the problems as follows:

- (1) In academia, most H₂ systems are designed to be installed in buildings, such as electrolyzers and H₂ tanks, whereas potential safety issues, such as the explosion of the high-pressured tank and conflagration due to flammable fuels, are rarely concerned. The geographical integration of H₂ systems in buildings is impractical and not acceptable for building owners. The transfer of a H₂ system from buildings to a H₂ station is an effective solution, especially considering the strict design regulations on H₂ stations [31], such as the mandatory security distance of large H₂ devices (like electrolyzers and large tanks) from ambient buildings. However, the current literature provides few studies on energy interaction and sharing between buildings, H₂ stations and mobile HVs.

- (2) Based on the rapid expansion on renewable electricity generation and distributed H₂ infrastructure, current residential communities are full of prospects and potentials in advancing regional carbon-neutral transition through transferring surplus renewable energy from buildings to vehicles. However, advanced energy control strategies for multiple energy interactions (electricity, thermal, and H₂ energy) among buildings, HVs, and H₂ stations, have been rarely explored in the H₂-supported district community. Furthermore, the capability through smart and flexible operation on associated H₂ devices to digest the intermittent renewable energy has been rarely investigated.
- (3) From the perspectives of multi-stakeholders in the H₂-based district energy community, the flexible power interaction among buildings, HVs, H₂ stations, and power grid can promote techno-economic benefits of multiple stakeholders. For example, switching surplus renewables from buildings to H₂ stations enhances renewable penetration into HVs and H₂ stations, and improves power grid stability due to the decrease in intermittent renewable congestion. The benefits of these stakeholders are not only decided by the prices of grid electricity and H₂, but also by the designed energy management strategies, which can be further optimized by setting proper parameters of the energy system, such as the input power of electrolyzers for H₂ production and the output power of vehicle PEMFCs for covering building energy demand. However, parametrical analysis on dynamic charging/discharging behavior is necessary to improve techno-economic benefits, so as to promote multiple stakeholders' participation.
- (4) The relevant previous studies usually ignored the idling modes of H₂-electricity devices, like electrolyzers and PEMFCs, in H₂-based energy networks [32], and assumed that electrolyzers and vehicle PEMFCs could freely start from the off status or be running at a very low power level. However, in practice, electrolyzers and PEMFCs have the idling modes, which are 10%-30% of the rated power to activate the electrochemical reactions and ensure the safe device operation [33]. Specifically, in the idling mode for electrolyzers, the minimum input power needed to be reached before starting the H₂ production process. In terms of the idling mode for PEMFCs, the demand shortage needs to be at least the minimum output power before it starts working. Otherwise, the current and voltage in the PEMFC stack will be too low to discharge the H₂. Compared to the single building integration with relatively low charging/discharging efficiency (due to low surplus energy to activate the electrolyzer system and low demand shortage to operate the fuel cell system when considering idling modes), the micro-grid-based district community integration can be an effective strategy to improve the performance of H₂ systems with high charging/discharging efficiency. The current literature provides limited studies to report the cutting-edge techniques towards the topic.
- (5) In respect to the exhaust heat recovery of PEMFC systems, another critical issue in the current academia is that, the cooling of PEMFCs was ideally simplified by normal water. Nonetheless, in practice, the cooling of PEMFCs relies on a closed loop filled with coolant. The released heat from the PEMFCs is absorbed by the coolant and then dissipated to the ambient environment through vehicle radiators. Such a feature requires to design a two-stage cooling system with a non-mixed heat exchanger for recovering the heat from the PEMFCs rather than directly using the coolant. There are few studies on the two-stage cooling system design for heat recovery from electrolyzers and PEMFCs, so as to improve the dynamic performance of electrolyzers and PEMFCs, together with the increase in recovered heat.

1.4 Research objectives

The hypothesis of this study is that the integration of residential buildings, H₂ stations, and fuel-cell-driven vehicles through electricity-H₂ and H₂-electricity conversion procedures, can have stronger energy independence, higher renewable penetration, and lower energy operating costs, and meanwhile reduce demand burdens on power grids and H₂

pipelines than when they are isolated from each other. This study aims to:

- (1) Propose practical energy management strategies for electricity-H₂ energy systems integrating residential buildings, H₂ stations, fuel-cell-driven vehicles, and other energy infrastructures, with considerations into fuel cell idling powers, and heat recovery from electrolyzers and fuel cells;
- (2) Explore multiple energy-related benefits for all stakeholders (including energy independence, grid power stability, energy operating costs, and so on) to promote the proposed novel energy system configuration and operation strategies.

The originalities of this study are summarized below:

- (1) Advanced energy management strategies which are for a regional hybrid electricity-H₂ energy system integrating residential houses, renewable energy systems, HVs, a H₂ station, local power grid, and local H₂ pipelines, with multiple energy interactions (electricity, H₂, and thermal energy) and advantages in energy flexibility, grid stability, and cost efficiency;
- (2) Practical considerations into H₂ storage security issue and idling modes of H₂ devices (electrolyzers and fuel cells), serving for the realistic practicability and feasibility of the proposed system;
- (3) Multiple energy interactions (electricity, H₂, and thermal energy) in the proposed energy system with synergistic functions between electrical battery and hydrogen storage systems to improve the energy efficiency;
- (4) Practical beneficial strategies for promoting stakeholders to participate in the proposed regional electricity-H₂ energy system.

To achieve the abovementioned research objectives, this study firstly establishes a hybrid electricity-H₂ district energy community integrating low-rise single houses, rooftop PV systems, HVs, a H₂ station with an electrolyzer and a compressor, local power grid, and local H₂ pipelines, located in California. Through deploying a community-based micro-grid connecting all houses, rooftop PV systems, a H₂ station, and HVs, the electricity-H₂ interaction is actualized by using the renewable electricity to activate the electrolyzer and compressor for H₂ production and by discharging the H₂ in the vehicle tanks via fuel cells for covering building demand. Besides, the thermal interaction among the buildings, vehicles, and H₂ station can be actualized by recovering the released heat from the electrolyzer when producing H₂ and from the vehicle PEMFCs to supply domestic hot water to the community houses. The first scientific gap can be filled, through the modeling development of the H₂-based district energy community. Moreover, multiple criteria of energy self-sufficiency, renewable penetration, grid interaction, energy consumption, and energy cost have been adopted to evaluate the energy system's performance under different energy management strategies, with considering the prices of local grid electricity and H₂ gas sold at local H₂ stations. Detailed benefits for the stakeholders' participation in the energy system, including the house owners, vehicle owners, H₂ station, and local power company, are analyzed, which fill the second and the third scientific gap above. Moreover, in addition to the single building-HV integration with relatively low charging/discharging efficiency (due to low surplus energy to activate the electrolyzer system and low demand shortage to operate the fuel cell system when considering idling modes), a micro-grid is formulated with peer-to-peer energy sharing in the district community to improve the performance of H₂ systems with high charging/discharging efficiency. This work fills the fourth scientific gap. In addition, the idling operating modes of the electrolyzer and vehicle PEMFCs are considered in the simulated energy system, and a unique two-stage cooling system of PEMFCs is built for heat recovery. This work fills the fifth scientific gap above. Furthermore, a parametric analysis on the input power of the electrolyzer and the output power of V2G interaction is conducted for balancing the annual grid stability and energy cost, which makes this research work more attractive and beneficial for potential stakeholders to promote their participation in the H₂-based district community with an integrated H₂ station.

2 Research case description

This section includes energy network parameters, network configuration, energy control strategies, simulation setup, assessment criteria, and so on.

2.1 Scenario, location, and climate

In this study, a residential community was studied, consisting of 30 single houses and 30 HVs, with a H₂ station nearby. The investigated community is located in the San Francisco Bay Area of California (namely, the Bay Area), the U.S.A, featuring cool winters with occasional rainfall and moderate summers [34].

The climate data for energy simulation herein is of San Francisco (37 °N, 122 °W). As shown in Fig. 3, the monthly mean outdoor temperatures are mainly between 10 and 16 °C, and the monthly mean outdoor relative humidity is mainly between 70% and 80%. Due to the cool climate, most local residential buildings only have space heating in winter but no space cooling in summer. Moreover, the local solar radiation and wind velocity have noticeable seasonal features: the monthly horizontal solar radiation is more than 200 kWh/m² from May to August, but it is less than 100 kWh/m² from November to February. The annual solar radiation is 1744 kWh/m², providing an enormous potential of utilizing renewable energy from solar radiation for the local residential buildings. Similarly, the local wind is relatively strong in summer, reaching more than 5 m/s from May to August, but it is relatively weak in winter, declining to less than 4 m/s from November to February.

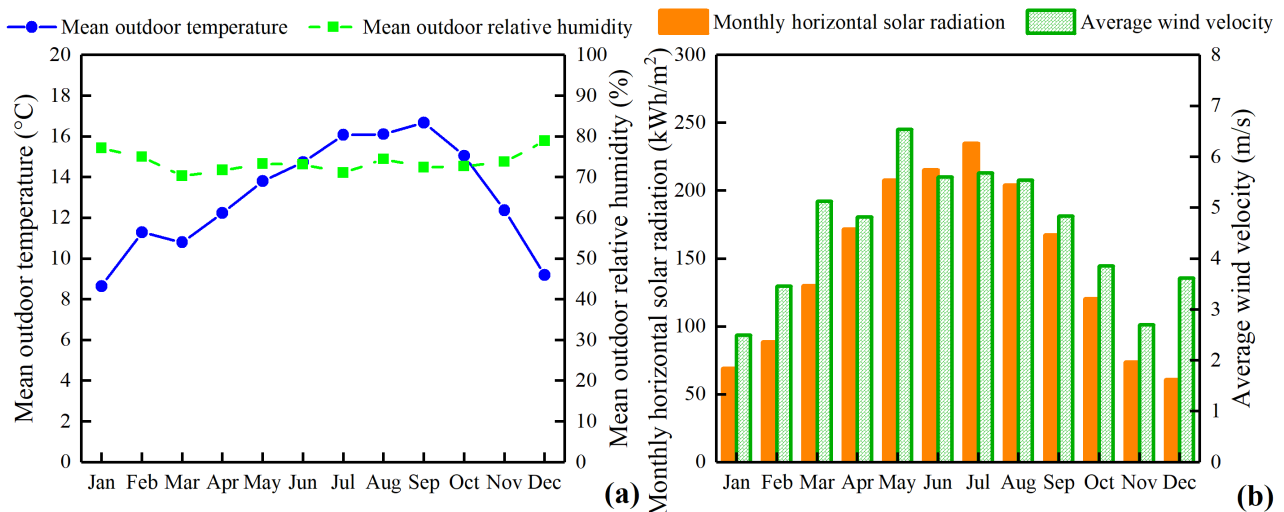


Fig. 3. Meteorological parameters of San Francisco: (a) mean outdoor temperatures and relative humidity, and (b) horizontal solar radiation and average wind velocity.

2.2 Buildings and roof photovoltaic systems

2.2.1 Overview

The community's buildings are low-rise single residential houses, which is common in the Bay Area. Each house has two floors with a 200-m² floor area (20 m × 10 m) for each floor (Fig. 4). The internal heights are 3.0 m and 4.5 m for the ground and second floors. The ground floor mainly includes a kitchen and living rooms, where most domestic electrical equipments are located, such as refrigerators, washing machines, dryers, dishwashers, cook ovens, and TVs. The second floor mainly consists of bedrooms and study rooms where the major electrical equipments are laptops and TVs. Each house's roof includes a flat surface and an inclined surface with a 45° tilted angle. The inclined roof surface is installed with 40-m² PV panels for generating renewable electricity (the detailed description of the PV panels is shown in section 2.2.4).

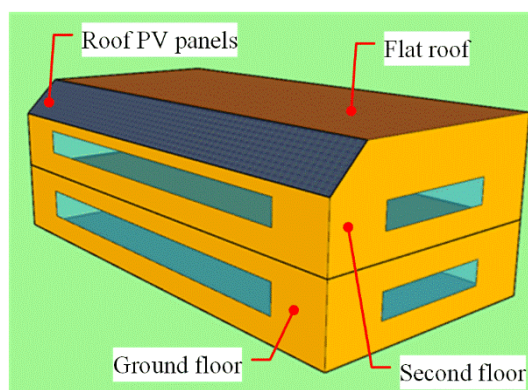


Fig. 4. The building geometry model.

The 30 single houses are divided into three groups (Building Groups 1, 2, and 3, respectively) with ten houses in each group, according to their different schedules of occupancy:

(1) In Building Group 1, each house has two occupants who leave their house (8:00-18:00) during weekdays and go out for several hours (9:00-12:00) during weekends. Building Group 1 represents two-people families whose members usually work from the office.

(2) In Building Group 2, each house has four occupants, of which two people leave their house (8:00-19:00) for a long time, and the rest two people leave their house for a short time (8:00-9:00 and 16:00-19:00) during weekdays. All family members go out during the daytime (9:00-18:00) on weekends. Building Group 2 represents four-people families that each family has (a) two parents working from home and two juveniles attending schools or (b) two members working from the office and two members working from home.

(3) In Building Group 3, each house has four occupants, of which three family members leave their house (8:00-18:00) during weekdays and go out for several hours (9:00-12:00) during weekends. Building Group 3 represents four-people families that each family has (a) a housewife who always stays at home or (b) a member working from home.

2.2.2 Building envelope parameters

For each floor, the south wall's window area is 15 m², and those of the north, east, and west windows are 5 m², with the total window area at 30 m². With the assumption that the whole house can be spatially heated in winter, the ratio of the window to the air-conditioned area is 15%, complying with the corresponding requirement of ASHRAE Standard 90.2 for energy-efficient design of low-rise residential buildings [35].

The houses' walls, floors, ceilings, and roofs mainly adopt light-weight materials, and the configuration of building envelopes is shown in Table 1. The solar heat gain coefficient (SHGC) values and U-values comply with the requirements of ASHRAE Standard 90.2 [35].

Table 1. Information of building envelopes.

Envelope	Configuration	Thickness (mm)	U-value (W/m ² K)	SHGC
Wall	10 mm plaster + 10 mm wood + 85 mm foam insulation +50 mm fibre glass + 10 wood + 10 mm plaster	175	0.262	-
Ceiling	25 mm timber + 5 wood + 200 mm foam insulation + 5 mm wood + 10 mm plaster	245	0.163	-

Ground floor	25 mm timber + 200 mm foam insulation + 300 mm concrete	525	0.178	-
Roof	10 mm plaster + 30 mm wood + 300 mm foam insulation + 50 fibre glass + 20 mm roof deck + 10 mm plaster	420	0.106	-
Window	6 mm glass + 16 mm air gap + 4 mm glass	6	1.01	0.22

2.2.3 Occupants, lighting, equipments, space heating, ventilation, and domestic hot water:

Occupants. In Building Groups 1, 2, and 3, each house has two, four, and four occupants, respectively. Every occupant indoors is assumed to have a 1.2-met metabolic rate (126 W), corresponding to the seated activities which are common during most of the time at home.

Lighting. For energy savings, the houses adopt high-efficiency lights with the efficacy ratio at 6, which means the that the lighting efficacy is 120 lm/W, more efficient than the required level of current standards such as ASHRAE Standard 90.2 [35]. And the corresponding largest internal heat gain from the artificial lighting indoors is set at 2 W/m².

Equipments. As described in section 2.2.1, in each house, the main domestic electrical equipments are placed on the ground floor, while the second floor has only a few equipments with low powers. Therefore, the largest internal heat gains from the equipments at the ground and the second floors are set as 15 and 5 W/m², respectively.

Space heating. The houses' space heating is actualized by electrical heaters, which are used from November to February. For the ground floor with living rooms, the indoor set-point temperature of space heating is set at 20 °C. For the second floor with bedrooms and study rooms, the set-point temperature of space heating is set at 18 °C.

Ventilation. In this study, the investigated houses have no mechanical ventilation systems (but some small devices like desktop fans and restroom fans are included). The fresh air supply of each house is mainly achieved by natural ventilation or air leak, for reducing energy consumption of mechanical ventilation systems. The air change rates (ACR) are set at 0.5 h⁻¹ when the outdoor temperature is beyond 20 °C and set at 0.1 h⁻¹ when the outdoor temperature is below 20 °C for saving the space heating energy. The ACR values comply with the requirements of ASHRAE Standard 62.2-2016 for residential building ventilation and air quality [36].

Domestic hot water. According to the energy-saving requirement of California, the supplied domestic hot water is expected to be at 49 °C (120 °F) [37]. In each house, the domestic hot water is produced by a tankless heater. The daily hot water consumption is set as 0.12 and 0.24 m³/day for a two-people house and a four-people house, respectively [38].

2.2.4 Rooftop photovoltaic systems

The houses adopt high-efficiency PV panels [39] with the reference efficiency of 0.22 under the standard testing condition, i.e., the solar radiation is 1000 W/m², and the reference temperature is 25 °C. The corresponding temperature coefficient is -0.3%/°C. The PV panels are installed on, and parallel to the inclined roof area, and thus the tilted angle of PV panels is 45°. The gap between the PV panels and the roof is 0.1 m to actualize the airflow's natural ventilation for cooling the PV panels. For each house, PV panels have a total area of 40 m², which reaches up to 94% of the inclined roof area. The size of each PV panel is 1.7 m × 1.0 m (length × width) with the unit price at about \$600 [40]. With California Solar Incentives [41], the PV panel purchase price can be lowered by 22%, and a total area of 40 m² consisting of 24 PV panels is \$11520 for each house.

2.3 Hydrogen vehicles

This study adopts a simplified HV model using parameters of the product “Toyota FCHV-adv” [42], whose maximum H₂ mass capacity, storage pressure, cruise distance after full-charging, and output power of the PEMFC are 6 kg, 700 bar, 690 km, and 90 kW, respectively.

Corresponding to the house groups described in Section 2.2, 30 HVs are divided into three groups (each group has ten HVs) with different schedules of parking near houses. The detailed parking schedule of each vehicle group is listed in Table 2. In Vehicle Group 1, HVs usually leave houses in the morning and park near houses at night, representing the vehicles owned by families whose members all work from the office during weekdays (corresponding to people of Building Group 1). In Vehicle Group 2, which corresponds to Building Group 2, during weekdays, HVs usually park near houses and only leave houses in the morning and afternoon for a short time; during weekends, HVs usually leave houses during the daytime. Like Vehicle Group 1, in Vehicle Group 3, which corresponds to Building Group 3, HVs usually park near houses at night.

Table 2. Information of the hydrogen vehicles.

	H ₂ tank capacity (kg/vehicle)	Period of vehicles parking in the community	Daily travel distance (km/vehicle)	H consumption (kg/km) ²
Group 1	6 [42]	Mon-Fri: 0:00-8:00, 18:00-24:00 Sat-Sun: 0:00-9:00, 12:00-24:00	50	0.0087 [42]
Group 2		Mon-Fri: 8:00-12:00, 9:00-16:00, 19:00-24:00 Sat-Sun: 0:00-9:00, 18:00-24:00	40	
Group 3		Mon-Fri: 0:00-8:00, 18:00-24:00 Sat-Sun: 0:00-9:00, 12:00-24:00	30	

In order to actualize the dynamic energy interaction of HVs in the model herein, some assumptions are made as follows:

(1) Each vehicle group is simplified as a storage system (a H₂ tank) and an energy consumer for transportation (a PEMFC, as listed in Table 4 for the detailed parameters).

(2) HV tanks can be charged at the H₂ station (a) one hour before HVs leave houses or (b) one hour after HVs come back to houses, corresponding to the fact that users charge HVs in the adjacent H₂ station just before traveling out or after traveling back.

(3) HV tanks are only discharged during transportation and V2G interaction processes. For transportation, the H₂ consumption of HVs is simplified and determined according to the actual distance, as shown in Table 2, without considering the difference in speed accelerating and decelerating processes.

(4) For the PEMFCs, the idling power is 18 kW, which is 20% of one HV's maximum power (90 kW). Moreover, from the perspectives of system operating efficiency, vehicles' safety issues and practicality, PEMFCs require a closed loop of coolant for removing the released heat rather than directly using normal water. Thus, for the V2G interaction (see Section 2.6), the heat recovered from PEMFCs for domestic hot water requires a two-stage cooling system: the first-stage cooling directly cools the PEMFCs by a closed-loop fulfilled with coolant (ethylene glycol solution including anti-electric-conduction ingredients); the second-stage cooling uses normal water to absorb heat from the coolant, after the coolant absorbs the heat from the PEMFCs. The heat transfer between the first and second stages is actualized through adopting a non-mixed heat exchanger.

(5) The lowest fractional state of charge (SOC) of HV tanks should ensure the pressure safety (tank pressure should be higher than the atmospheric pressure, and it is at least 2 bar herein) and support at least one-day transportation energy demand (as shown in Table 2). Therefore, the lowest SOC of HV tanks (the lower SOC limit, i.e., SOC_{lower, limit})

is 0.08, meeting the requirements of one-day transport demand and pressure safety. If the SOC_{lower, limit} is lower than 0.08, HVs will be charged to the SOC level at 0.95 (the upper SOC limit, i.e., SOC_{upper, limit}) at the H₂ station before traveling out or after traveling back. The SOC_{lower, limit} of HV tanks is also the threshold for the V2G interaction, which means that V2G interaction can only be activated when the SOC of HV tanks is higher than 0.08.

The detailed model parameters for actualizing the abovementioned assumptions are listed in Table 4.

2.4 Hydrogen station

Currently, in California, there are 42 already developed H₂ stations available for public HVs charging, and there are 15 H₂ stations in development [27]. A typical H₂ station is capable of dispensing 100-400 kg H₂ per day, and the fuel-charging of each HV needs less than five minutes [43]. In this study, the H₂ station adjacent to the investigated community is assumed to dispense 100 kg H₂ per day for supporting regional transportation. The H₂ station is assumed to be supplied with H₂ gas by the local H₂ pipelines, with the proportion of renewable-produced H₂ at 33% [44]. Moreover, the H₂ price for charging HVs is \$16.51 per kg [45].

In this study, in order to actualize the integration of the community and H₂ station, a H₂ system, consisting of an electrolyzer with the maximum power of 200 kW for H₂ production and a compressor for compressing the produced H₂ to 700 bar, is added in the H₂ station. The H₂ system only produces H₂ gas using onsite renewable electricity from the houses' integrated rooftop PV systems, making the onsite produced H₂ become 100% renewable. Therefore, for the H₂ station, there are two sources of H₂: (1) one is from the electrolyzer in the H₂ station, in which H₂ is produced by 100% renewable energy from the building integrated rooftop PV systems; (2) the other one is from the local H₂ pipelines, in which H₂ is produced by 33% renewable energy and 67% non-renewable energy [44].

Moreover, for the electrolyzer, the idling power is 40 kW, which is 20% of its maximum input power. Namely, the input electric power for generating H₂ should be at least 40 kW. Besides, the maximum capacity of the H₂ station for storing the onsite-renewable-produced H₂ is set at 1000 kg. Furthermore, during the H₂ production, the heat released by the electrolyzer is recovered through a hydraulic system. The detailed design information on warmed cooling water and warmed cooling water of the second-stage cooling system of PEMFCs is described in Section 2.3. The recovered heat is stored in a 6-m³ tank and used for covering part of domestic hot water heating load of the community. The key parameters of the H₂ system are listed in Table 4.

2.5 Grid information

This study selects the Time-of-Use Plan (E-Tou-D) of the Pacific Gas and Electric Company (i.e., PG&E) [46], which is the major local electrical company in the Bay Area. This plan defines the peak and off-peak periods: the peak period is 17:00-20:00 during weekdays, and the rest time is the off-peak period. This plan adopts different energy prices for the two periods, as shown in Table 3. Meanwhile, the PG&E has a solar energy project for compensating the electricity bill [47]. A house with PV panels can compensate the grid-imported electricity cost by exporting PV-generated electricity to the grid with the prices listed in Table 3, but only before the annual grid-imported electricity cost is fully compensated. In other words, if a house with PV panels exports more electricity than the imported electricity from the grid within a year, the house owner will not be paid by the electric grid, but receive an additional reward from the government, depending on the amount of net surplus electricity exported to the grid at the price of \$0.03 per kWh [48].

Table 3. Cost information on the local grid in the Bay Area.

Month	Electricity rate (\$/kWh)		Annual net surplus electricity reward (\$/kWh)
	Peak period	Off-peak period	0.03

Jun-Sep	0.36540	0.27044
Jan-May & Oct-Dec	0.29153	0.27415

2.6 Energy system configuration and management strategies

Fig. 5 illustrates the structural configuration of the proposed district H₂-based energy network, consisting of houses, HVs, H₂ station, local power grid, and local H₂ pipelines. The PV panels installed on the houses are the major renewable energy sources for the district community, reducing the grid dependence for demand coverage of buildings, and decreasing the reliance on H₂ delivered by the local pipelines for transportation demand coverage of vehicles. The renewable electricity generated by the rooftop PV panels is used to cover the building energy demand, and the surplus renewable electricity is exported into the community micro-grid (B2G interaction). The H₂ system (the electrolyzer and compressor) at the H₂ station is connected to the micro-grid and can converse the surplus renewable electricity to H₂ gas (G2S interaction), which is then stored in the H₂ station. The H₂ at the H₂ station is used to charge HV tanks (S2V interaction). Vehicle PEMFCs can discharge the H₂ stored in HV tanks to support daily transportation or power the micro-grid connecting the community's houses (V2G interaction). Meanwhile, when the electrolyzer generates H₂ (G2S interaction) or the PEMFCs discharge H₂ for powering the micro-grid (V2G), the heat released by the electrolyzer or the PEMFCs is recovered by cooling water, which is then stored in a water tank to cover domestic hot water heating demand. Moreover, the community micro-grid is connected to the local power grid, which dynamically balances the micro-grid through absorbing surplus renewable electricity and covering demand shortage. The H₂ station is connected to the local H₂ pipelines that supply H₂ to support regional transportation demand (not only the HVs of the community).

Through the configuration of such an energy system, the renewable electricity generated by the rooftop PV panels meets building energy demands during the daytime and covers the energy demand for daily transportation of the HVs. Furthermore, the onsite-renewable-produced H₂ can be discharged by HVs to cover the building demand shortage. Therefore, the local grid has a decreased burden for supporting electric demand of the community and lowered grid congestion for absorbing intermittent renewable electricity from the rooftop PVs in the community. With the abovementioned energy interactions, the community can achieve high energy flexibility and grid power stability.

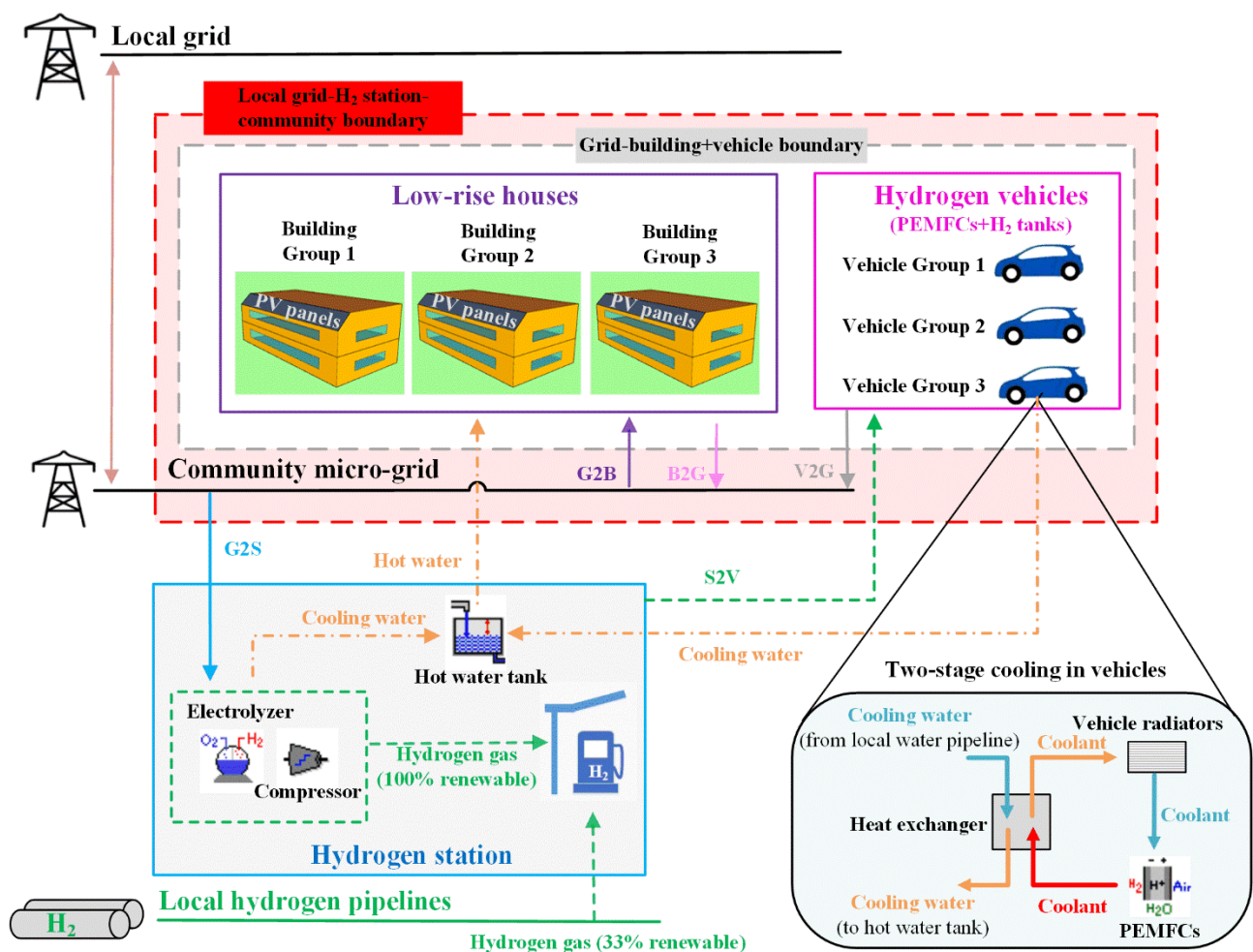


Fig. 5. The structural configuration of a community integrating low-rise residential buildings, rooftop PV systems, fuel-cell-powered HVs, an adjacent H₂ station, local hydrogen pipelines, community micro-grid, and local power grid. (G2B means the grid-to-building interaction; B2G means the building-to-grid interaction; G2S means the grid-to-H₂-station interaction; S2V means the H₂-station-to-vehicle interaction; V2G means the vehicle-to-grid interaction.)

The underlying mechanism and working principle of the district energy community is shown below. On the one hand, after being directly managed to cover building demand, the surplus renewable electricity from onsite renewable systems can be absorbed by H₂ systems, instead of being exported to the power grid. The H₂ systems convert renewable electricity into H₂ gas to be stored in H₂ stations. The stored H₂ gas will charge HVs for daily transportation. On the other hand, the stored onsite-renewable-produced H₂ can be discharged by vehicle PEMFCs for building demand coverage. Furthermore, during the processes of producing H₂ and H₂ tanks discharging for the V2G interaction, the chemical reaction heat can be recycled from electrolyzers and PEMFCs of HVs, enabling the coverage of domestic hot water systems of buildings. More importantly, compared to the limited storage volume of H₂ systems installed in buildings (for the security concerns), H₂ stations are able to provide much larger storage capacities for storing the renewable-generated H₂ and enhancing energy flexibility.

Four energy management strategies are proposed herein, including one simple strategy as the reference case and three other advanced strategies. The detailed control logics of the four cases are represented as follows:

(1) Reference case (Fig. 6(a)): the community has isolated houses, HVs, and a H₂ station nearby, without any energy interactions. This case is designed to represent normal communities without an internal micro-grid. Namely, each house is individually connected to the local grid. To be more specific, for each house, the renewable electricity from the

rooftop PV panels is only used by the house itself or exported to the local grid, without being shared by other houses or the H₂ station. The HVs are only charged at the H₂ station with H₂ delivered by the local H₂ pipelines.

As shown in Fig. 6(b), the renewable electric power ($P_{REe, i}$) of the i -th house firstly covers its building energy demand ($L_{e, i}$):

a) If $P_{REe, i}$ is higher than $L_{e, i}$, the surplus renewable of the i -th house ($P_{REe, surpl, i} = P_{REe, i} - L_{e, i}$) is exported to the local grid.

b) If $P_{REe, i}$ is lower than $L_{e, i}$, the energy shortage of the i -th house ($P_{short1, i} = L_{e, i} - P_{REe, i}$) is covered by the local grid.

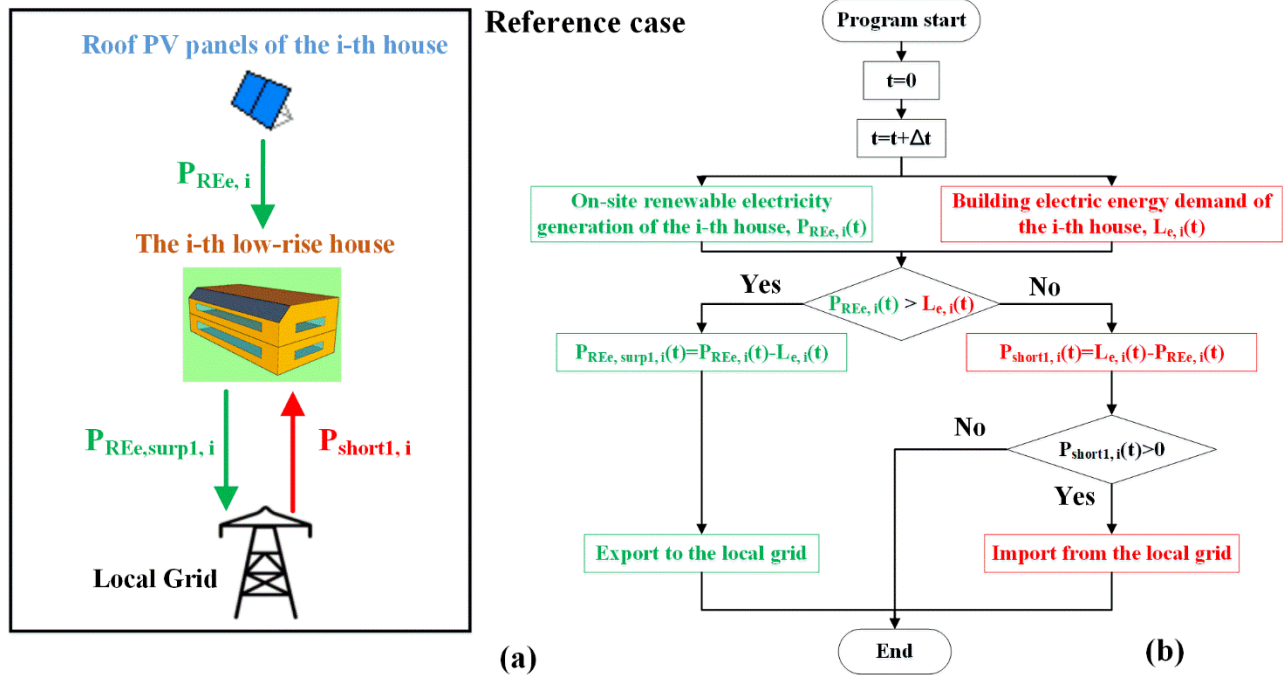


Fig. 6. (a) Energy flow and (b) control logic of the reference case.

(2) Case 1 (Fig. 7(a)): The community has a micro-grid connecting all houses and rooftop PV systems, but it is not connected to the H₂ station. This case is designed to represent some communities where houses share the micro-grid for making the best use of onsite renewables, such as those under the EcoBlock project in California [49]. As compared to the reference case where the houses connect to the local grid separately, Case 1 has a community micro-grid that neutralizes the renewables and energy demands of all the houses in the community before it connects to the local grid. In Case 1, the whole community's renewable electric power (P_{REe}) is the sum of renewable powers of all the houses, and the building energy demand of the whole community (L_e) is the sum of energy demands of all the houses. Owing to the micro-grid, the renewable electric power (P_{REe}) firstly covers the building energy demand (L_e) (Fig. 7(b)):

a) If P_{REe} is higher than L_e , the surplus renewable ($P_{REe, surpl} = P_{REe} - L_e$) is exported to the local grid.

b) If P_{REe} is lower than L_e , the energy shortage ($P_{short1} = L_e - P_{REe}$) is covered by the local grid.

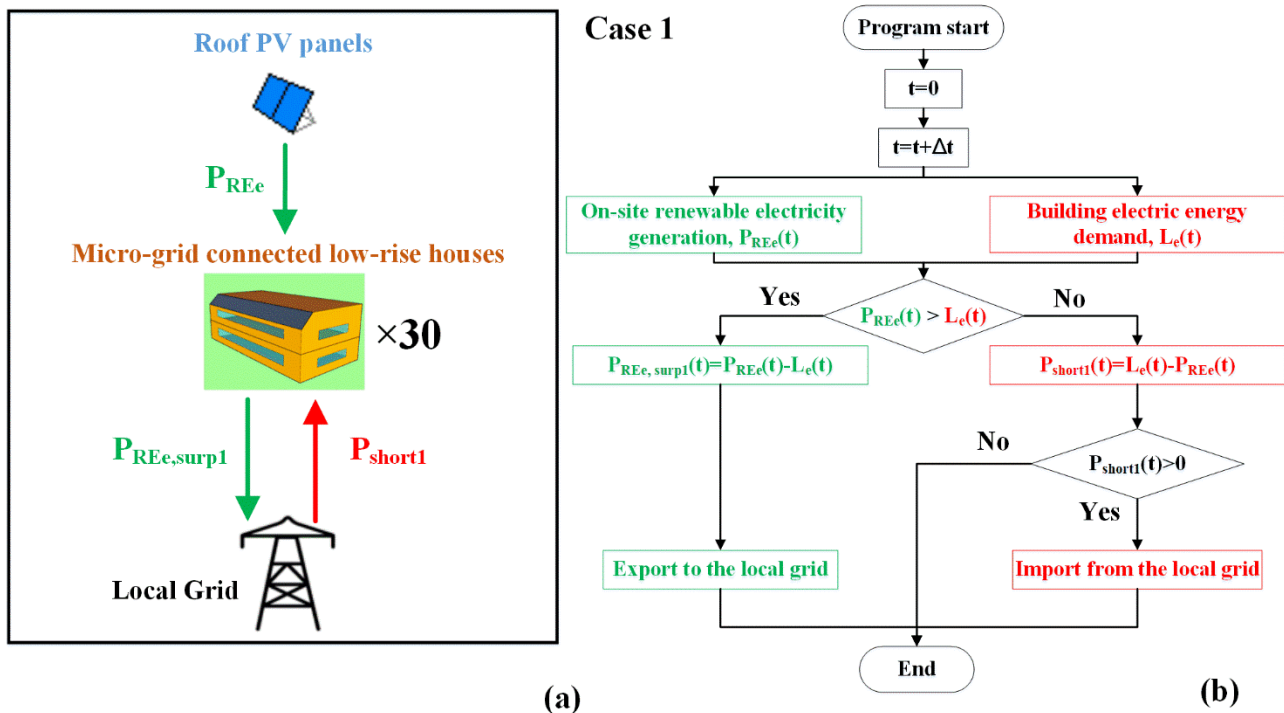


Fig. 7. (a) Energy flow and (b) control logic of Case 1.

(3) Case 2 (Fig. 8(a)): The community has a micro-grid connecting all houses, rooftop PV systems, and the H₂ station. The renewable electricity can power the electrolyzer and compressor in the H₂ station for producing H₂ gas. Compared to Case 1, in Case 2, the micro-grid connecting to the H₂ station enables the community's surplus renewables to penetrate daily transportation energy use. Such a feature reduces the pipe-delivered H₂ in the H₂ station and mitigates the grid's renewable congestion during the midday when PV panels generate enormous electricity. For the community, the renewable electric power (P_{REe}) still firstly covers the building energy demand (L_e) (Fig. 8(b)):

a) If P_{REe} is higher than L_e , the surplus renewable of the community ($P_{REe, surp1} = P_{REe} - L_e$) is exported to the H₂ system at the H₂ station or the grid, depending on the magnitude of $P_{REe, surp1}$. Specifically, if $P_{REe, surp1}$ is lower than the sum of the electrolyzer idling power ($P_{ely, idling}$) and the compressor power (P_{comp}), the $P_{REe, surp1}$ is exported to the local grid, as the surplus energy fails to activate the electrolyzer system. If $P_{REe, surp1}$ is higher than the sum of the electrolyzer idling power ($P_{ely, idling}$) and the compressor power (P_{comp}), and meanwhile in the previous dynamic status, the accumulated amount of H₂ charged to the HVs of the community ($H_{2charged}$) is higher than the accumulated amount of onsite-renewable-produced H₂ ($H_{2produced}$) by the renewable electricity from the community, $P_{REe, surp1}$ will be still sent to the electrolyzer and compressor for H₂ production which is then stored in the H₂ station. If $P_{REe, surp1}$ is higher than the sum of the electrolyzer idling power ($P_{ely, idling}$) and the compressor power (P_{comp}), and meanwhile in the previous dynamic status, the $H_{2produced}$ (by renewables of the community) reaches up to the $H_{2charged}$ (to the HVs of the community), $P_{REe, surp1}$ will be still sent to the local grid. Furthermore, if the $P_{REe, surp1}$ is higher than the sum of the powers of the electrolyzer (P_{ely}) and the compressor (P_{comp}), the exceeded renewable ($P_{REe, surp2}$) is exported to the local grid.

b) If P_{REe} is lower than L_e , the energy shortage ($P_{short1} = L_e - P_{REe}$) is covered by the local grid.

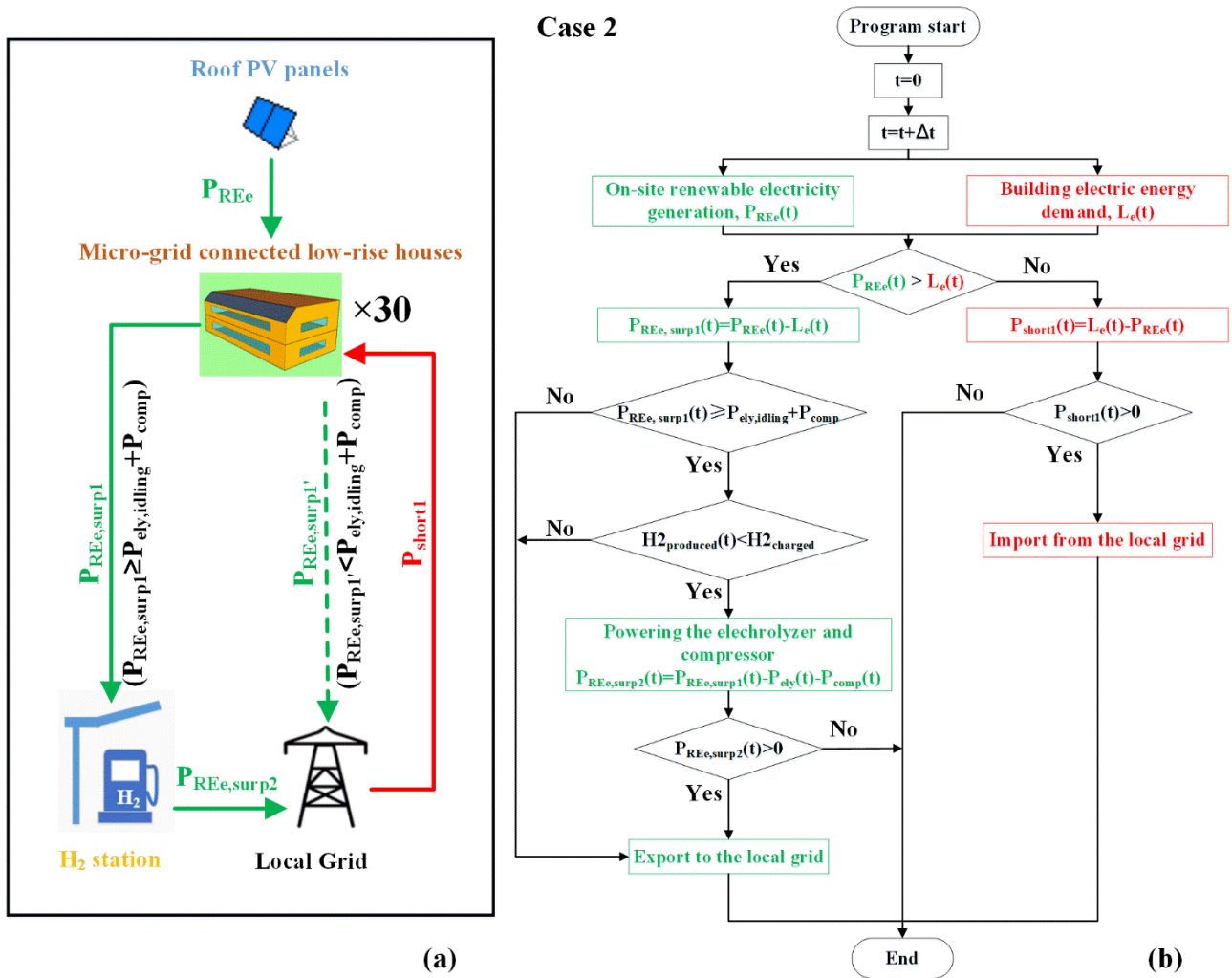


Fig. 8. (a) Energy flow and (b) control logic of Case 2.

(4) Case 3 (Fig. 9(a)): The strategy is similar to that of Case 2, but the onsite-renewable-produced H₂ can be discharged by the PEMFCs of HVs for powering the houses (V2G interaction). With the added V2G interaction, the HVs play a role as the energy consumer in the community and as the energy storer for enhancement of energy flexibility and grid stability. After the renewable electric power (P_{REe}) covers the building energy demand (L_e) (Fig. 9(b)):

a) If P_{REe} is higher than L_e , the surplus renewable of the community ($P_{REe, surp1} = P_{REe} - L_e$) has the same energy flow route as that of Case 2, but the renewable electricity can be sent to the H₂ system before the stored onsite-renewable-generated H₂ mass ($H_{2RE, store}$) at the H₂ station reaches the storage limit of the onsite-renewable-generated H₂ ($H_{2RE, store, limit} = 1000$ kg in Case 3).

b) If P_{REe} is lower than L_e , the energy shortage ($P_{short1} = L_e - P_{REe}$) is covered by the discharged power of vehicle PEMFCs ($P_{H2, dischar}$) only when the fractional state of charge of HV tanks (SOC_{HV}) is higher than $SOC_{lower, limit}$, $H_{2RE, store}$ is higher than zero, and P_{short1} is higher than the idling power of a PEMFC ($P_{FC, idling}$) simultaneously. Otherwise, P_{short1} is covered by electricity imported from the grid. Moreover, if P_{short1} is higher than the available $P_{H2, dischar}$, the rest of the energy shortage ($P_{short2} = P_{short1} - P_{H2, dischar}$) is covered by the local grid.

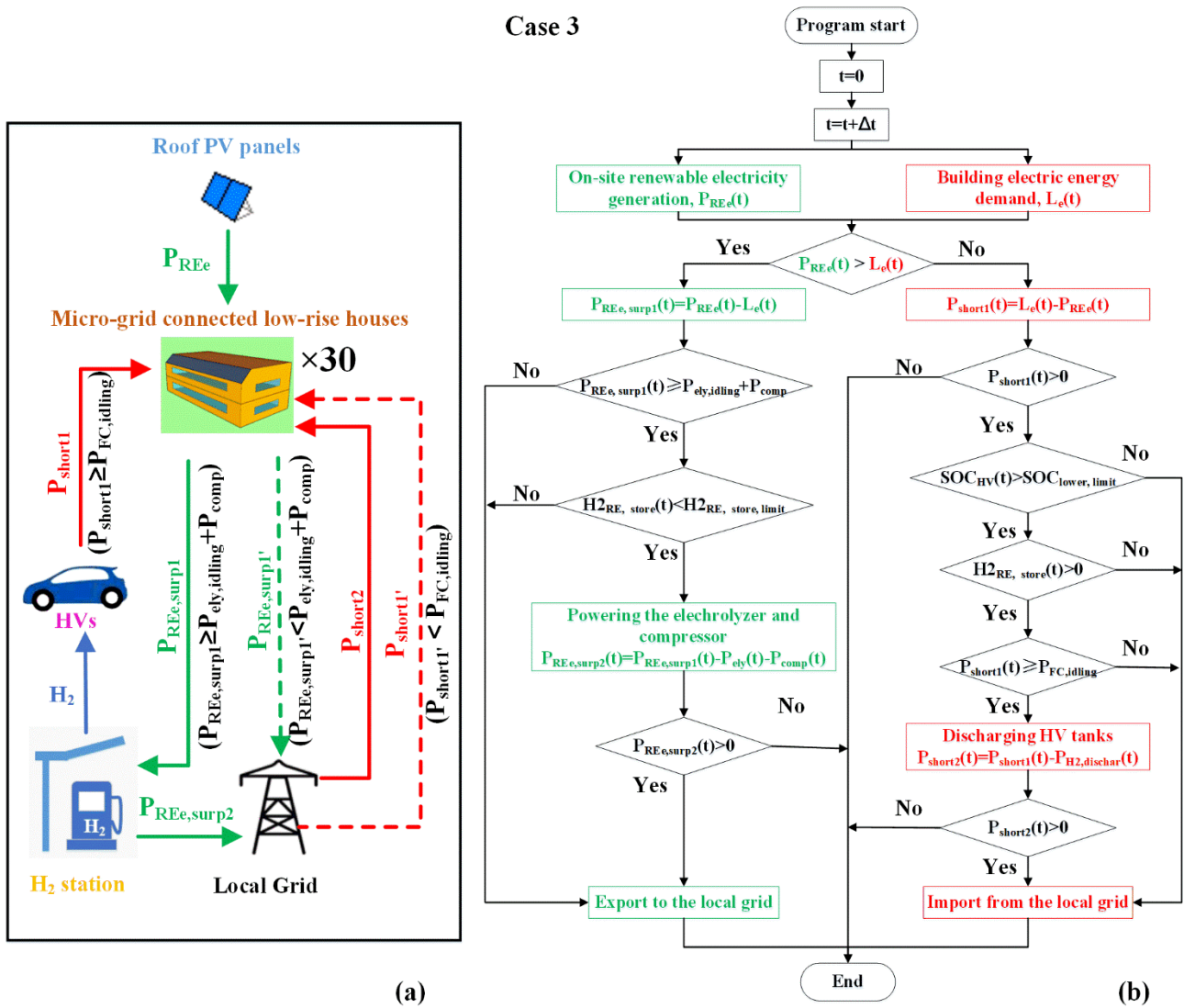


Fig. 9. (a) Energy flow and (b) control logic of Case 3.

3 Methods

The methods mainly include the energy simulation establishment and assessment criteria for evaluating the performance of the proposed energy system.

3.1 Energy simulation model establishment

Herein, TRNSYS 18 [50] is adopted for transient energy simulations of the integration of houses, HVs, and H₂ station. The time step of the simulation is set at 0.25 h. The parameters of models representing components of the integration of houses, HVs, and H₂ station are listed in Table 4. The corresponding energy management strategies in the proposed cases (see Section 2.6) are built in the TRNSYS script.

Table 4. Key parameters of the energy system.

Components	Parameters	Values
PV panels	Type in TRNSYS 18	567
	Collector length (m)	20
	Collector width (m)	2
	Channel height (m)	0.1
	Reference PV efficiency	0.22
	Temperature coefficient (/°C)	-0.003
Electrolyzer	Type in TRNSYS 18	160a
	Electrode area (m ²)	0.5
	Number of cells per stack	20
	Number of stacks	2
	Cooling water inlet temperature (°C)	20
	Cooling water flow rate (m ³ /h)	0.6
	Operating temperature (°C)	80
Compressor	Type in TRNSYS 18	167
	Number of parallel compressors	1
	Number of compressor stages	3
	Desired pressure (bar)	700
HV hydrogen tank (for each group)	Type in TRNSYS 18	164b
	Maximum pressure (bar)	700
	Tank volume (m ³)	1.51
PEMFC	Type in TRNSYS 18	170d
	Number of cells per stack	80
	Number of stacks	20
	Electrode area (cm ²)	500
	Coolant inlet temperature (°C)	30
	Coolant temperature rise (°C)	25
H ₂ station	Type in TRNSYS 18	Self-developed
	Daily dispensing H ₂ (kg/day)	100
	Maximum stored onsite-renewable-produced H ₂ (kg)	1000
	Renewable penetration ratio of pipeline-delivered H ₂	0.33
Domestic tankless heater	Type in TRNSYS 18	138
	Maximum heating rate (kW)	80
	Set-point temperature (°C)	49

Heat exchanger (for two-stage cooling)	Type in TRNSYS 18	5
	Load side inlet temperature (°C)	20
	Overall heat transfer coefficient (W/K)	2000
Water tank	Type in TRNSYS 18	39
	Overall tank volume (m ³)	6
	Tank circumference (m)	10
	Cross-sectional area (m ²)	6
	Wetted loss coefficient (kJ/h·m ² ·K)	1.5
	Wetted loss coefficient (kJ/h·m ² ·K)	1.0

3.2 Assessment criteria

The assessment criteria used in this study involve the system performance in terms of energy self-sufficiency, renewable penetration, grid interaction, energy consumption, and energy cost.

3.2.1 Energy self-sufficiency and renewable penetration

The annual energy self-sufficiency ratio (*SSR*) is the fraction of annual building energy demand covered by renewables ($0 \leq SSR \leq 1$) [51]. If *SSR* is 1, 100% of the building energy demand is covered by renewables rather than by electricity imported from the grid. In this study, the *SSR* is extended to the annual energy self-sufficiency ratio of buildings (*SSR_{building}*) and the annual energy self-sufficiency ratio of HVs (*SSR_{HVtran}*). *SSR_{building}* is the fraction of annual building energy demand covered by renewables or other stored energy rather than the grid-imported electricity ($0 \leq SSR_{building} \leq 1$). If *SSR_{building}* is 1, 100% of the building energy demand is covered by renewables or other stored energy rather than by grid-imported electricity. *SSR_{HVtran}* is the fraction of the annual transportation energy demand of HVs covered by the H₂ produced by renewable electricity from the PV-integrated houses rather than H₂ imported from the local H₂ pipeline ($0 \leq SSR_{HVtran} \leq 1$). If *SSR_{HV}* is 1, 100% of the annual transport energy demand of HVs is covered by the onsite-renewable-produced H₂. *SSR_{building}* and *SSR_{HVtran}* are calculated as follows:

$$SSR_{building} = \frac{\int_0^{t_{end}} \text{Min}[P_{REe}(t) + P_{V2G}(t) + P_{DHW, stored}(t), L_e(t)] dt}{\int_0^{t_{end}} L_e(t) dt} \quad (1)$$

$$SSR_{HVtran} = \text{Min} \left\{ \frac{\int_0^{t_{end}} [M_{RE, H2, building}(t) - M_{V2G, H2}(t)] dt}{\int_0^{t_{end}} M_{HVtran, H2}(t) dt}, 1 \right\} \quad (2)$$

where $P_{REe}(t)$ is the electrical power of renewables at the t -th time step (kJ/h); $P_{V2G}(t)$ is the electrical power of V2G interaction at the t -th time step (kJ/h); $P_{DHW, stored}(t)$ is the reduced power of domestic hot water heaters by the stored hot water which is produced by cooling the electrolyzer or the PEMFCs at the t -th time step (kJ/h); $L_e(t)$ is the electrical power of building energy demand at the t -th time step (kJ/h); $M_{RE, H2, building}(t)$ is the H₂ produced by renewable electricity from the PV-integrated houses at the t -th time step (kg/h); $M_{V2G, H2}(t)$ is the H₂ consumed by vehicle PEMFCs for powering the micro-grid (V2G interaction) at the t -th time step (kg/h); $M_{HVtran, H2}(t)$ is the H₂ consumed by vehicle PEMFCs for transportation at the t -th time step (kg/h); Min is the minimum function; t is the time step (h). t_{end} is the end time of the simulation, which is the 8760th hour in this study.

As described in Section 2.4, the H₂ of the H₂ station comes from two sources: (1) the renewable driven H₂ through

the electricity-to-H₂ conversion process from the rooftop PVs in the community; (2) the pipeline-delivered H₂ from the local pipelines, which is produced by 33% renewable energy (renewable-to-H₂ conversion) and 67% non-renewable energy (such as syngas-to-H₂ conversion). In order to characterize the ratio of the renewable driven H₂ to the total H₂ dispensed by the H₂ station, the renewable penetration ratio of the H₂ station ($RPR_{station}$) is proposed and shown in Eq. (3). If $RPR_{station}$ ($0 \leq RPR_{station} \leq 1$) is 1, it means that all the dispensed H₂ by the H₂ station is produced by renewable energy. Moreover, in order to characterize the ratio of the transportation energy demand of HVs covered by renewables, the renewable penetration ratio of HVs (RPR_{HVtran}) is proposed and shown in Eq. (4). If RPR_{HVtran} ($0 \leq RPR_{HVtran} \leq 1$) is 1, it means that all the H₂ consumed by the HVs of the community for daily transportation is produced by renewable energy. The $RPR_{station}$ and RPR_{HVtran} can provide information on the carbon-neutral level of local H₂ station and local transportation systems.

$$M_{RE, H_2, pipe}(t) = 0.33 \times [M_{station, H_2}(t) - M_{RE, H_2, building}(t)] \quad (3)$$

$$RPR_{station} = \frac{\int_0^{t_{end}} M_{RE, H_2, building}(t) dt + \int_0^{t_{end}} M_{RE, H_2, pipe}(t) dt}{\int_0^{t_{end}} M_{station, H_2}(t) dt} \quad (4)$$

$$M_{net, RE, H_2, building}(t) = M_{RE, H_2, building}(t) - M_{V2G, H_2}(t) \quad (5)$$

$$RPR_{HVtran} = 1 - \frac{\text{Max} \left\{ 0.67 \times \int_0^{t_{end}} [M_{HVtran, H_2}(t) - M_{net, RE, H_2, building}(t)] dt, 0 \right\}}{\int_0^{t_{end}} M_{HVtran, H_2}(t) dt} \quad (6)$$

where $M_{RE, H_2, pipe}(t)$ is the renewable-produced H₂ delivered by pipelines from remote H₂ plants and dispensed by the H₂ station (kg/h); $M_{station, H_2}(t)$ is the H₂ dispensed by the H₂ station (kg/h), which includes the H₂ for V2G interaction; $M_{net, RE, H_2, building}(t)$ is the net H₂ produced by renewable electricity from the PV-integrated houses at the t -th time step (kg/h); Max is the maximum function.

3.2.2 Grid interaction

In this study, the electric grid absorbs the surplus renewable electricity and powers the houses when it is an energy demand shortage. The intensities of grid importation and exportation are evaluated by the import and export powers (P_{imp} for the grid-imported power and P_{exp} for the grid-exported power), respectively. A low P_{imp} value indicates the low burden of the grid powering the investigated community. A low P_{exp} value indicates the low renewable congestion of the grid absorbing PV-generated electricity.

3.2.3 Annual net energy consumption and cost

The annual net electricity consumption of the investigated community is calculated as follows:

$$E_{imp} = \int_0^{t_{end}} P_{imp}(t) dt \quad (7)$$

$$E_{exp} = \int_0^{t_{end}} P_{exp}(t) dt \quad (8)$$

$$E_{net, annual} = E_{imp} - E_{exp} \quad (9)$$

where E_{imp} and E_{exp} are the annual imported and exported electricity, respectively (kWh/a); $E_{net, annual}$ is the annual net electricity consumption (kWh/a). Owing to the fact that the grid-imported electricity is only for the coverage of building demands herein, if $E_{net, annual}$ is higher than zero, it indicates that the houses need more grid-imported electricity than the

grid-exported electricity within one year. Otherwise, the houses achieve the net ZEBs ($E_{net, annual} = 0$) or even export more electricity to the grid than the imported electricity ($E_{net, annual} \leq 0$).

From the perspective of district residential buildings in the community, the annual net H₂ consumption of HVs (including H₂ use for both daily transportation and V2G interaction) is calculated as follows:

$$H_{consume, annual} = \int_0^{t_{end}} [M_{tran, H_2}(t) + M_{V2G, H_2}(t)] dt \quad (10)$$

$$H_{produce, annual} = \int_0^{t_{end}} M_{RE, H_2, building}(t) dt \quad (11)$$

$$H_{net, annual} = H_{consume, annual} - H_{produce, annual} \quad (12)$$

where $H_{consume, annual}$ is the annual consumed H₂ (kg/a); $H_{produce, annual}$ is the annual produced H₂ by renewable electricity from the buildings in the community (kg/a); $H_{net, annual}$ is the annual net H₂ consumption (kg/a). If $H_{net, annual}$ is higher than zero, it indicates that the community consumes more H₂ than the H₂ produced by onsite renewables within one year.

The total energy cost of the investigated community consists of the costs of electricity and H₂. According to the grid information described in Section 2.5, the annual cost by the grid-imported electricity (IC , \$/a) and the annual compensation by the grid-exported electricity (EC , \$/a) are calculated as follows:

$$IC_{peak, mon, i} = E_{imp, peak, mon, i} \times R_{peak, mon, i} \quad (13)$$

$$IC_{off-peak, mon, i} = E_{imp, off-peak, mon, i} \times R_{off-peak, mon, i} \quad (14)$$

$$IC = \sum_{i=1}^{12} (IC_{peak, mon, i} + IC_{off-peak, mon, i}) \quad (15)$$

$$EC_{peak, mon, i} = E_{exp, peak, mon, i} \times R_{peak, mon, i} \quad (16)$$

$$EC_{off-peak, mon, i} = E_{exp, off-peak, mon, i} \times R_{off-peak, mon, i} \quad (17)$$

$$EC = \sum_{i=1}^{12} (EC_{peak, mon, i} + EC_{off-peak, mon, i}) \quad (18)$$

where $E_{imp, peak, mon, i}$ and $E_{imp, off-peak, mon, i}$ are the grid-imported electricity quantities during the peak period and the off-peak period of the i -th month, respectively (kWh/month); $R_{peak, mon, i}$ and $R_{off-peak, mon, i}$ are the grid electricity prices during the peak period and the off-peak period of the i -th month, respectively (\$/kWh), and the detailed prices are listed in Table 3; $IC_{peak, mon, i}$ and $IC_{off-peak, mon, i}$ are the costs by the grid-imported electricity quantities during the peak period and the off-peak period of the i -th month, respectively (\$/month); $E_{exp, peak, mon, i}$ and $E_{exp, off-peak, mon, i}$ are the grid-exported electricity quantities during the peak period and the off-peak period of the i -th month, respectively (kWh/month); $EC_{peak, mon, i}$ and $EC_{off-peak, mon, i}$ are the compensations by the grid-imported electricity quantities during the peak period and the off-peak period of the i -th month, respectively (\$/month).

The electricity cost by the grid-imported cost and grid-exported compensation ($C_{e, 1}$, \$/a) is calculated as follows:

$$C_{e, 1} = \begin{cases} IC - EC & \text{if } IC > EC \\ 0 & \text{if } IC \leq EC \end{cases} \quad (19)$$

The additional reward due to the annual net electricity consumption ($C_{e, 2}$, \$/a) is calculated as follows:

$$C_{e,2} = \begin{cases} (-E_{\text{net, annual}}) \times 0.03 & \text{if } E_{\text{net, annual}} < 0 \\ 0 & \text{if } E_{\text{net, annual}} \geq 0 \end{cases} \quad (20)$$

Therefore, the total annual electricity cost (C_e , \$/a) is calculated as follows:

$$C_e = C_{e,1} - C_{e,2} \quad (21)$$

Currently, there is no information about the compensation price of H₂ produced by renewables. The H₂ is 16.51 \$/kg [45]. Herein, the annual cost of H₂ (C_{H2} , \$/a) is simply calculated according to the annual net H₂ consumption of HVs:

$$C_{H2} = \begin{cases} H_{\text{net, annual}} \times 16.51 & \text{if } H_{\text{net, annual}} > 0 \\ 0 & \text{if } H_{\text{net, annual}} \leq 0 \end{cases} \quad (22)$$

The total annual energy cost (C_{energy} , \$/a) is calculated as follows:

$$C_{\text{energy}} = C_e + C_{H2} \quad (23)$$

3.3 Simulation errors

The main results of this study are obtained through simulations. The simulation error (E_{error}) is evaluated according to the energy imbalance of the proposed community:

$$E_{\text{error}} = \frac{\left| \int_0^{t_{\text{end}}} P_{\text{REe}}(t) dt + \int_0^{t_{\text{end}}} P_{\text{fromH2}}(t) dt + E_{\text{imp}} - \int_0^{t_{\text{end}}} L_e(t) dt - \int_0^{t_{\text{end}}} P_{\text{toH2}}(t) dt - E_{\text{exp}} \right|}{\int_0^{t_{\text{end}}} P_{\text{REe}}(t) dt + E_{\text{imp}}} \quad (24)$$

where $P_{\text{fromH2}}(t)$ is the electrical power from the vehicle PEMFCs at the t -th time step (kJ/h); $P_{\text{toH2}}(t)$ is the electrical power sent to the H₂ system in the H₂ station at the t -th time step (kJ/h).

In this study, E_{error} is lower than 0.01% in each case, indicating that the energy balance can be reached and simulation results are reliable.

4 Results

In this section, Section 4.1 presents energy demand and production of the proposed community. Section 4.2 presents the energy-related performance. Section 4.3 presents the parametric optimization of the H₂ system. Section 4.4 presents the summarized benefits of the optimized energy management strategy.

4.1 Energy demand and renewable generation of the community

Fig. 10 illustrates the monthly total building electricity demand, equipment electricity demand (lighting, devices, and hot water heating, but not including space heating), space heating demand, PV-generated electricity, and H₂ consumption for vehicle transportation of the investigated community. The monthly building electricity demand is relatively large in winter, reaching up to 1244.4 kWh per household in January. It is relatively small in other months without space heating, reaching about 600 kWh per household. The total annual building electricity demand is 8769.1 kWh per household. The monthly PV-generated electricity is 1100-1300 kWh per household from April to September but declines to about 700 kWh per household in winter. The annual PV-generated electricity reaches 12271.5 kWh per household. Moreover, the annual total H₂ use for daily transportation is 127.0 kg per vehicle, supporting the annual total travel distance of 14600 km per vehicle. Furthermore, it is noteworthy that the annual PV-generated electricity is much higher than the annual building electricity demand, providing the considerable potential for using surplus renewable to cover the energy demand of daily transportation.

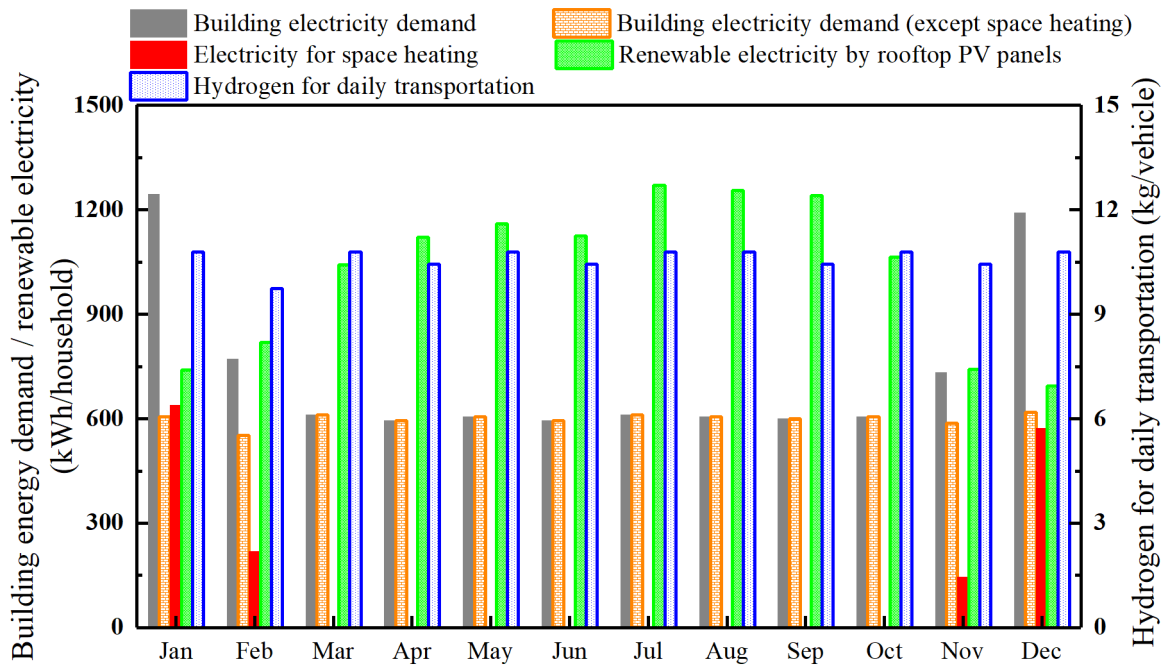


Fig. 10. Monthly energy demand and renewable generation per household of the investigated community.

4.2 Impact of energy planning and management strategy on techno-economic performance, energy flexibility, and grid power stability

4.2.1 Energy self-sufficiency and renewable penetration of houses and vehicles

Fig. 11 shows the impact of energy management strategies on the energy self-sufficiency rates and the renewable penetration rates. As shown in Fig. 11(a), compared to other three cases, in Case 3 (the integrated community and H₂ station with V2G interaction), the houses show the highest energy self-sufficiency ratio at 0.406, with the annual demand-matched renewable/stored energy and the annual building demand at 3.85×10^8 kJ and 9.47×10^8 kJ, respectively. Specially, the V2G interaction provides 7.61×10^7 kJ electricity to the community, covering 8% of the total energy demand. The reference case has the lowest $SSR_{building}$ at 0.229 (annual demand-matched renewable/stored electricity at 2.17×10^8 kJ vs. annual building demand at 9.47×10^8 kJ). In Cases 1 and 2, the $SSR_{building}$ values are 0.240 and 0.284, respectively (the amounts of annual demand-matched renewable/stored energy are 2.27×10^8 kJ and 2.69×10^8 kJ, respectively). Besides, Case 3 (the integrated community and H₂ station with V2G interaction) shows the highest energy self-sufficiency rate of HVs among the four cases. In the reference case and Case 1, due to the isolated community from the H₂ station, the SSR_{HVtran} is at zero, which indicates that all the H₂ charged to the HVs is from the local H₂ pipelines. In Case 2, the integration of the community and H₂ station actualizes an SSR_{HVtran} value at 0.984 (annually, 3746.9 kg onsite-renewable-produced H₂ vs. 3808.7 kg H₂ for the daily transportation of the HVs), indicating that 98.4% of the H₂ for the daily transportation is produced by the renewable electricity from the PV systems installed on the house roofs. Compared to Case 2, in Case 3, 3771.3 kg of 5006.6 kg onsite-renewable-produced H₂ is used for covering transportation energy demand, which results in the SSR_{HVtran} at 0.990.

As shown in Fig. 11(b), in Case 3, the H₂ station has the highest renewable penetration rate. In the reference case and Case 1, due to the isolated community from the H₂ station, $RPR_{station}$ is at 33%, the same as the renewable ratio of the pipe-delivered H₂ at the H₂ station. In Case 2, 3746.9 kg of the total 36500 kg dispensed H₂ is 100%-renewable produced by the community's renewable electricity (201995.2 kWh community renewable electricity is consumed by

the electrolyzer running for 1476 hours, and the electricity-H₂ conversion efficiency is about 63.5%), resulting in the $RPR_{station}$ at 0.399. In Case 3, 5006.6 kg of the total 37735.2 kg dispensed H₂ is 100%-renewable produced by the community's renewable electricity, resulting in the $RPR_{station}$ at 0.430. Similarly, in Case 3, the 30 HVs have the highest renewable penetration into their transportation energy. In the reference case and Case 1, due to the isolated community from the H₂ station, the H₂ charged to the HVs is totally pipe-delivered, and thus RPR_{HVtran} is the same as $RPR_{station}$ (33%). In Case 2, 3746.9 kg of 3808.7 kg H₂ for the annual transportation energy demand of the HVs is 100%-renewable, and the rest H₂ is from the pipeline with the renewable ratio at 33%. Therefore, RPR_{HVtran} is 0.989 in Case 2. In Case 3, 3771.3 kg of 3808.7 kg H₂ for the annual transportation energy demand is 100%-renewable (270999.4 kWh community renewable electricity is consumed by the electrolyzer running for 2333 hours, and the electricity-H₂ conversion efficiency is about 63.5%), and the rest H₂ is 33%-renewable, resulting in the RPR_{HVtran} at 0.993.

To summarize, the results in Fig. 11 indicate that compared to the reference case, the integration of the community and H₂ station with V2G interaction (Case 3) is the best option for energy self-efficiency and renewable penetration. With the implementation of Case 3, the houses and HVs actualize energy self-sufficiency rates at 40.6% and 99.0%, respectively, and the renewable penetration rates of the H₂ station and HVs at 43.0% and 99.3%, respectively. In other words, the formulated Case 3 with peer-to-peer energy sharing, district community-based micro-grid, H₂-based interactive energy sharing network and integration of local H₂ station, can promote the carbon-neutral community with high self-sufficiency of renewable energy and high renewable penetration levels in both buildings and transportations.

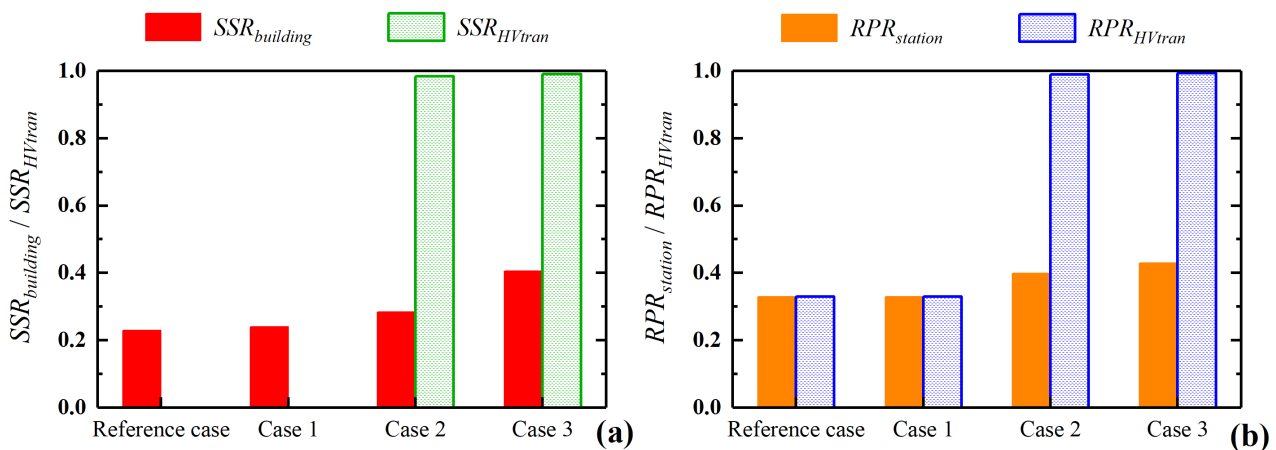


Fig. 11. Impacts of different energy management strategies on (a) energy self-sufficiency and (b) renewable penetration.

4.2.2 Grid power stability

Fig. 12 illustrates the dynamic grid power under the four energy management strategies. The values are mean hourly grid powers (positive values for grid-import powers and negative values for grid-export powers), which are mean values of the grid powers at a certain time point of a day during the non-space-heating period or space-heating period.

Among the four cases, the community and H₂ station's integration with V2G interaction in Case 3 is the best solution for reducing grid burden (grid-import power) and renewable congestion (grid-export power). During the non-space-heating period (Fig. 12(a)), Case 3 shows the lowest grid-export power during the daytime (15.0 kW at most) and the lowest grid-import power during the nighttime (50.7 kW at most), which is significantly superior to other three cases (the maximum mean hourly grid-export powers are 149.5, 149.5, and 31.4 kW in the reference case, Cases 1, and Case 2, respectively; and the maximum mean hourly grid-import powers are 86.5, 86.5, and 83.1 kW in the reference case, Cases 1, and Case 2, respectively.). During the space-heating period (Fig. 12(b)), due to the increased building energy demand and decreased PV electricity (as shown in Fig. 10), fewer renewables are stored in the form of H₂ gas, which is

later discharged for covering building demands. Therefore, compared to other cases, Case 3 shows minimal advantages of covering building demand at night. The maximum mean hourly grid-import powers in the four cases are the same at 103.2 kW. The maximum grid-export powers are 103.0, 103.0, 26.1, and 4.8 kW in the reference case and Cases 1-3, respectively. Therefore, the community and H₂ station's integration is the best case in terms of grid power stability.

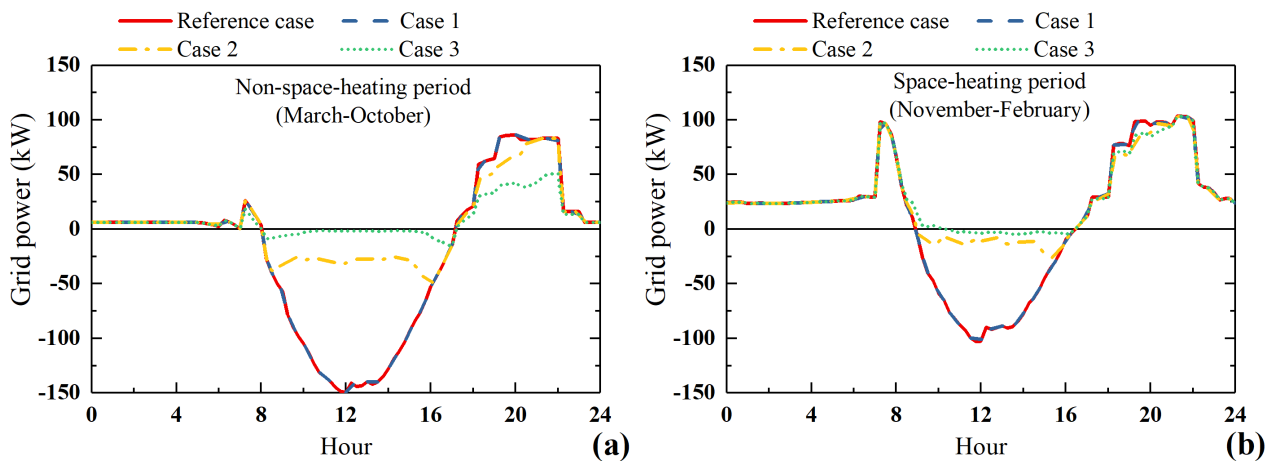


Fig. 12. Grid power of the integrated community and H₂ station under different energy management strategies: (a) non-space-heating period and (b) space-heating period.

4.2.3 Annual net energy consumption and economic cost

Fig. 13 illustrates the annual net consumption of grid electricity and H₂, and the corresponding costs under different energy management strategies. In Fig. 13(a), the positive values of the net grid electricity mean that the community consumes more grid-imported electricity than the grid-exported electricity, while the negative values mean that the community has more grid-exported electricity than the grid-imported electricity. The integration of the community and H₂ station (Cases 2 and 3) has much higher net grid electricity consumption (3457.1 kWh/household and 4656.5 kWh/household) than the isolated community and H₂ station in the reference case and Case 1 (both cases are -2888.8 kWh/household). Meanwhile, since the renewable electricity is converted into H₂ (3746.9 and 5006.6 kg in Cases 2 and 3, respectively) for covering transportation energy demand, the integration of the community and H₂ station with V2G interaction in Case 3 has the lowest annual net H₂ consumption at 1.2 kg/vehicle, followed by the integration of the community and H₂ station without V2G interaction in Case 2 (2.1 kg/vehicle). Moreover, due to the isolated community and H₂ station in the reference case and Case 1, the net H₂ consumption is 127.0 kg/vehicle, much higher than those in Cases 2 and 3 (2.1 and 1.2 kg/vehicle, respectively).

Corresponding to the results of annual net energy consumption, as shown in Fig. 13(b), the integration of the community and H₂ station significantly increases the grid electricity cost but lowers the annual H₂ cost, and the combined grid electricity and H₂ cost needs to be investigated. Compared to the reference case (2009.4 \$/household), forming a shared micro-grid of the community in Case 1 does not reduce the electricity cost, as the H₂ cost is 2096.1 \$/vehicle either in the reference case or Case 1, indicating that the cost of daily transportation is 0.144\$/km. Since much renewable electricity is released into the H₂ system in Cases 2 and 3, the electricity costs of Cases 2 and 3 rise up to 1008.9 and 1308.7 \$/household, respectively. Meanwhile, the H₂ costs of Cases 2 and 3 are reduced to 34.0 and 20.6 \$/vehicle, respectively, meaning that daily transportation costs are reduced to 0.002 and 0.001 \$/km, respectively. As a result, compared to the reference case, the annual energy costs of Cases 2 and 3 are reduced by 48.1 and 38.9% for each household, respectively.

It is noteworthy that the integration of the community and H₂ station with V2G integration in Case 3 has higher net

electricity consumption than other cases without V2G interaction. Such a result is caused by (1) the less compensated grid electricity in Case 3, and (2) the low energy efficiency of the electricity-H₂-electricity conversion procedure (40-50%). For point (1), for example, although the V2G interaction in Case 3 reduces the grid-imported electricity to 5205.1 kWh/household from that at 6758.4 kWh/household in the reference case, Case 3 has much less grid-exported electricity for compensating the cost of the grid imported electricity (548.6 kWh/household in Case 3 vs. 9647.2 kWh/household in the reference case). From another perspective, the V2G interaction in Case 3 will increase the energy loss due to the low efficiency of the H₂-to-electricity conversion process, and the increased energy loss during the energy interaction process can also be noticed in electrical battery systems [52, 53]. The annual net used grid-imported electricity is still higher in Case 3 than in the reference case, which finally increases the net electricity consumption in Case 3. For point (2), even though V2G interaction is adopted, the overall electricity efficiency of the electricity-H₂-electricity conversion procedure (G2S and V2G interaction) is about 40-50%. Although part of the waste heat during this procedure is recovered, there is a large energy loss, and the energy storage efficiency is still relatively low. Therefore, much grid electricity is still needed to cover building demands, which elevates the energy cost in Case 3.

To summarize, the results in Fig. 13 indicate that compared to the reference case, the integration of the community and H₂ station without V2G interaction is the most economical strategy, reducing the total energy cost by 48.1%. The deployment of only a community micro-grid does not reduce the community's annual energy cost, and the integration of the community and H₂ station with V2G interaction reduces the total energy cost by 33.9%.

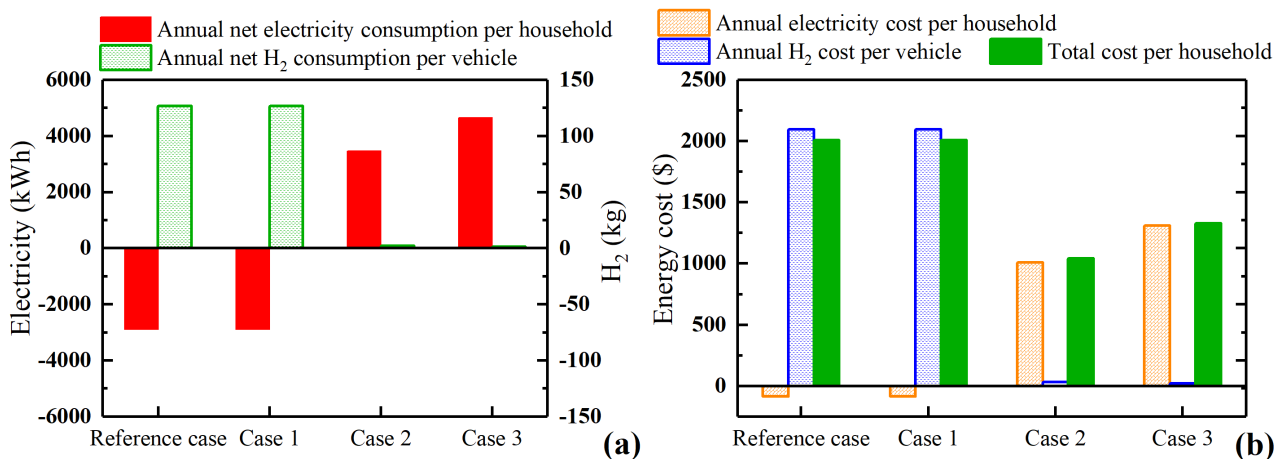


Fig. 13. Comparative analysis between different energy management strategies, in terms of (a) annual net energy consumptions; (b) annual energy costs of the integrated community and H₂ station.

4.3 Parametric optimization on flexible charging power in electrolyzer and discharging power in fuel cell

According to the results of Section 4.2, the integration of the community and H₂ station with V2G interaction (Case 3) can promote the carbon-neutral community with high self-sufficiency of renewable energy and high renewable penetration levels in both buildings and transportations, together with grid power stability. However, two main problems are still not solved:

(1) The integration of community and H₂ station with V2G interaction does not significantly reduce the grid peak power in winter due to the high energy demand and the low threshold of output power (idling power of PEMFCs at 18 kW) for V2G interaction. To be more specific, from the seasonal perspective, in summer, when the solar radiation is sufficient during the daytime, the low threshold of output power for V2G interaction discharges the stored H₂ (produced during the daytime) for covering building energy demand at night. As a result, an enormous amount of the onsite-renewable-produced H₂ is consumed in summer. Only a little is stored over seasons and available for V2G interaction during the space-heating period in winter.

(2) Although the integration of community and H₂ station with V2G interaction in Case 3 shows promising benefits in terms of energy self-sufficiency, renewable penetration, and grid stability, Case 3 does not significantly reduce the total energy cost of each household, compared to Case 2 (the integration of community and H₂ station without V2G interaction). This problem will undoubtedly block the application of V2G interaction in practice.

The abovementioned problems might be solved by properly elevating the minimum output power of V2G interaction (V2G_{min}) for covering building demand and the minimum input power of the electrolyzer for H₂ production (Ely_{min}).

(1) The flexible adjustment on the magnitude of V2G_{min} can actualize the seasonal energy storage of H₂ storage. To be specific, the increase of the V2G_{min} can reduce the H₂ discharged for the building demand coverage during the low power period (such as the non-space-heating period). Thus, more onsite-renewable-produced H₂ can be discharged for the building demand coverage during the peak period (such as the space-heating period).

(2) By adjusting the Ely_{min}, the cost of grid electricity can be reduced. To be more specific, elevating the lowest input power for activating the electrolyzer will reduce the renewable electricity absorbed by the electrolyzer for H₂ production and increase the renewable electricity injected into the local grid for compensating the grid cost (see Section 2.5).

The parametric optimization herein adopts the integration of community and H₂ station with V2G interaction (Case 3). The assessment criteria of grid interaction and energy cost are used for analyzing the effects of the critical parameters.

4.3.1 The effect of the output power of vehicle-to-grid interaction

Initially, the V2G_{min} is the idling power of PEMFCs of HVs (18 kW) in Case 3. For the demonstration purpose and future perspective with advanced development in PEMFCs technologies, the V2G_{min} is set at 60-110 kW with an increasing step of 10 kW.

Fig. 14(a) and Fig. 14(b) illustrate the mean hourly grid powers with different V2G_{min} values. Apparently, elevating the minimum V2G power increases the grid-import power during the non-space-heating period and reduces the grid-import power during the space-heating period. Specifically, during the non-space-heating period, when the V2G_{min} increases from 60 to 90 kW, the maximum mean hourly grid-import power increases from 55.2 to 83.1 kW; if the V2G_{min} increases from 90 to 110 kW, the maximum mean hourly grid-import power keeps unchanged at 83.1 kW. Meanwhile, when the V2G_{min} increases from 60 to 90 kW, the maximum mean hourly grid-import power decreases from 103.2 to about 60 kW; if the V2G_{min} continues to go up from 90 to 110 kW, the maximum grid-import in winter increases from about 60 kW to 80 kW since the V2G interaction with the over-increased V2G_{min} covers less energy demand. For example, when V2G_{min} is set at 80 kW, the V2G interaction covers more than 18000 kWh of the building demand annually; but it only covers less than 6400 kWh of the building demand when the V2G_{min} is set at 110 kW. Moreover, elevating the minimum V2G power does not significantly increase the grid-export power in the non-space-heating or space-heating period.

Fig. 14(c) illustrates the energy cost with different V2G_{min} values. Obviously, elevating the V2G_{min} does not vastly change each household's annual energy cost, with the total energy cost reaching about 1350 \$/household. It is noteworthy that when the V2G_{min} increases from 70 to 110 kW, at the end of the year, the amount of onsite-renewable-H₂ left in the H₂ station without being used increases from 27.2 to 493.3 kg, indicating that the stored H₂ is underuse. However, due to the cost calculation rule herein (see section 3.2), the unused left onsite-renewable-H₂ at the H₂ station does not compensate for the total energy cost. Therefore, the total energy cost is not reduced with the increased V2G_{min} and the unused H₂.

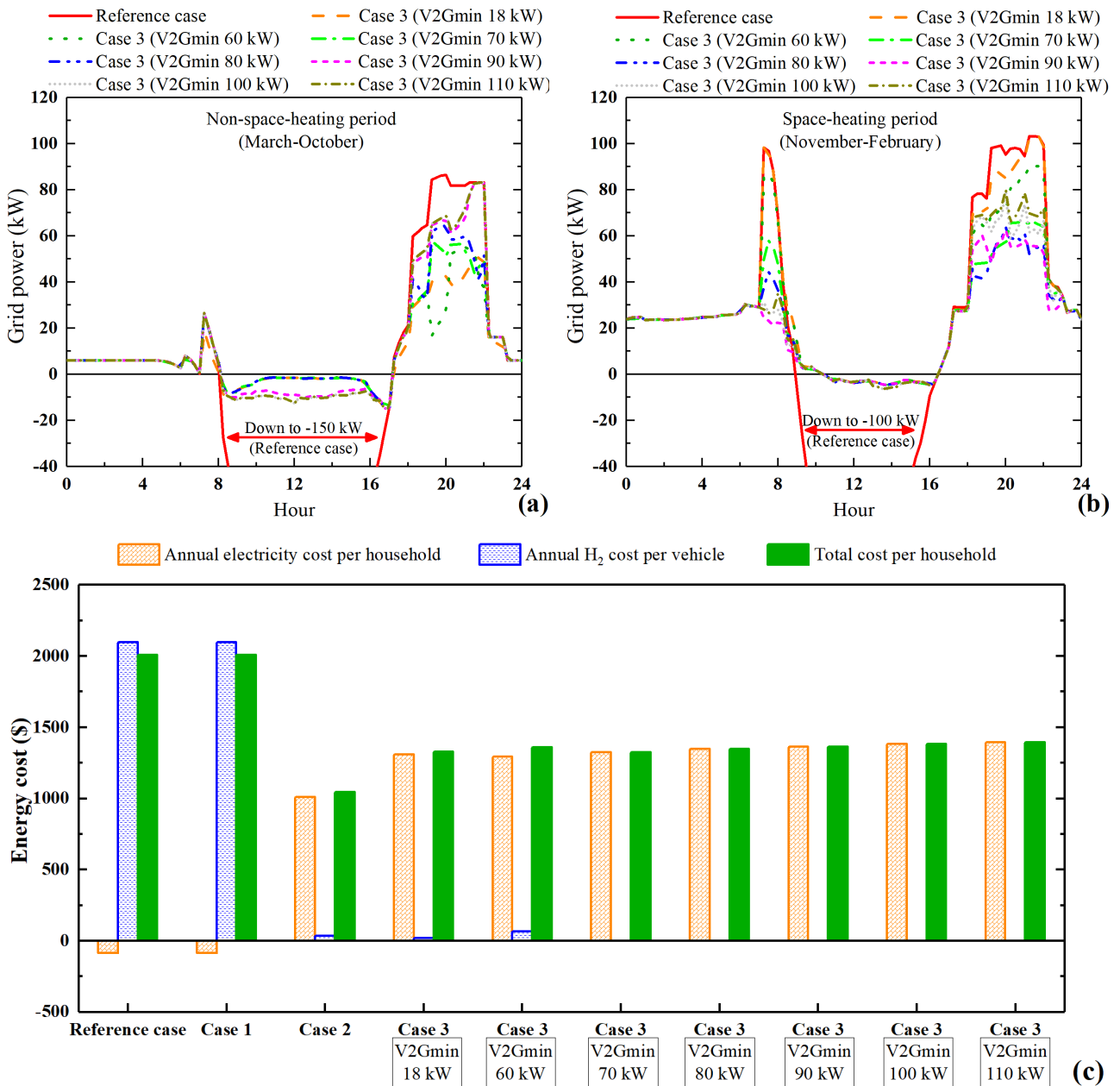


Fig. 14. The effects of the lower threshold of V2G power for covering building demands on grid powers during (a) non-space-heating period and (b) space-heating period and on (c) annual energy costs.

4.3.2 The effect of the input power of electrolyzer for hydrogen production

According to the results of Fig. 14, it can be found that the lowest output power of V2G interaction at 80 kW reduces the mean hourly grid-import powers to about 70 and 60 kW during the non-space-heating and space-heating periods, respectively, exerting a promising effect on the seasonal energy storage for annual grid stability. Therefore, the lowest output power of V2G interaction is set at 80 kW in this section to exclusively analyze the effects of the electrolyzer input power.

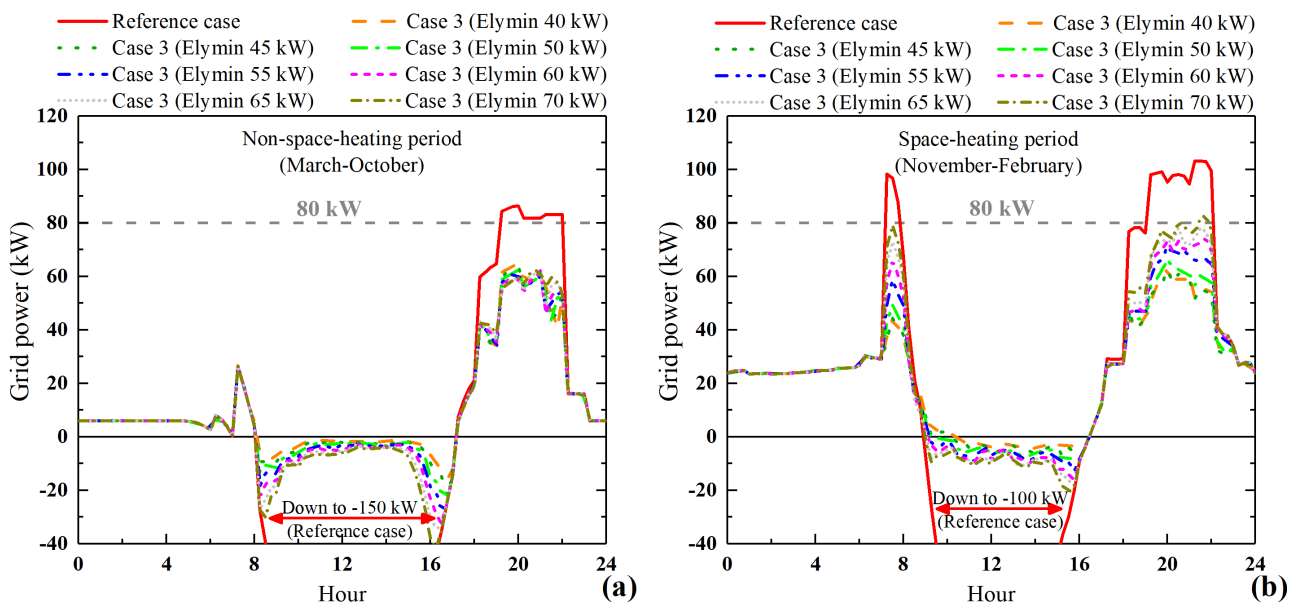
Initially, the Elymin is the idling power of the electrolyzer (40 kW). Here, it is set at 40-70 kW with an increasing step of 5 kW.

Fig. 15(a) and Fig. 15(b) illustrate the mean hourly grid powers with different Elymin values. Apparently, elevating the Elymin slightly increases the grid-export power during the daytime and the maximum grid-import power during the

space-heating period. Specifically, during the non-space-heating period, when the Elymin increases from 40 to 70 kW, the maximum mean hourly grid-export power increases from about 20 to 40 kW. During the space-heating period, the maximum mean hourly grid-export power increases from about 8 to 20 kW. Meanwhile, when the Elymin increases from about 40 to 70 kW, the maximum mean hourly grid-import power during the non-space-heating period almost stays unchanged at around 60 kW. During the space-heating period, the maximum grid-import increases from about 60 kW to 80 kW.

Fig. 15(c) illustrates the energy cost with different Elymin values. Elevating the Elymin reduces the annual energy cost of each household. When the Elymin increases from 40 to 70 kW, the annual energy cost decreases from 1346.9 \$/household to 1208.1 \$/household. The reduction of the annual energy cost can be attributed to the reduction of the net grid electricity consumption. To be specific, when the Elymin increases from 40 to 70 kW, the annual net grid electricity consumption decreases from 4742.4 kWh/household to 4113.6 kWh/household, which results in a reduction in the grid electricity cost. Meanwhile, the annual H₂ cost is still low, reaching 34.4 \$/vehicle at most.

Furthermore, it is noteworthy that the case with the minimum input power of the electrolyzer at 65 kW and the minimum power of V2G interaction at 80 kW can be regarded as a good balance for the annual grid stability and energy cost. With the identified parameter setting, the maximum grid power is 78.2 kW, which is 24.2% lower than that in the reference case. Meanwhile, each household's annual energy cost is 1228.5 \$, which is 38.9% less than that in the reference case.



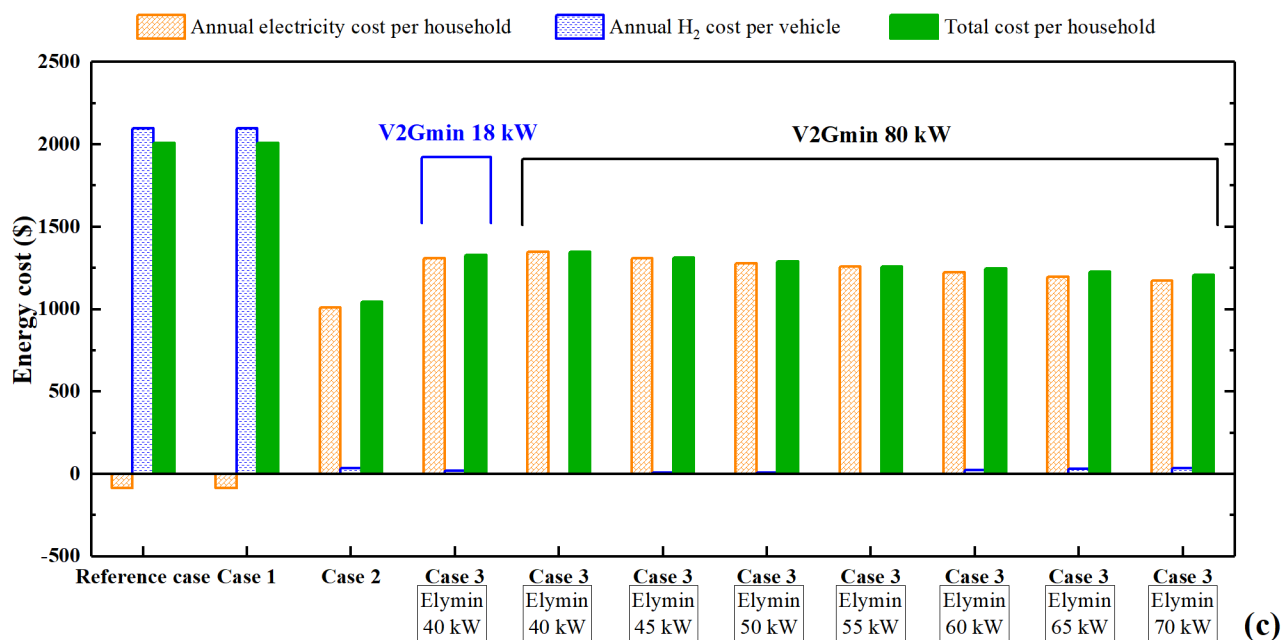


Fig. 15. The effects of the lower threshold of electrolyzer input power for H₂ production on grid powers during (a) non-space-heating period and (b) space-heating period; and on (c) annual energy costs.

4.4 A summary of the benefits for multiple stakeholders by integrating a hydrogen station

The promising results of enhanced energy flexibility in the studied H₂-based district energy community with advanced energy management strategies can provide a multilateral-win situation for all stakeholders participating in the H₂-station-integrated regional energy system. Table 5 summarizes the enhanced energy flexibility and practical techno-economic benefits of the H₂-based district energy community.

(1) For the house owners, the most crucial benefit is the reduced total energy cost through the transfer of surplus renewables from buildings to vehicles via the dynamic renewable-to-gas energy conversion process. Another potential benefit for integrating a H₂ station is the reduced power of domestic hot water heaters due to the two-stage cooling system for heat recovery, which saves domestic hot water systems' initial cost in practice.

(2) For the HV owners (usually also the house owners), the most crucial benefit is the reduced cost of daily transportation through the increased self-sufficiency rate using the onsite-renewable-produced H₂ to charge HVs. The improved renewable penetration of transportation energy can reduce CO₂ emission and environmental pollution from the transportation sector.

(3) For the local grid, mitigated pressure imposed by intermittent renewable energy integration can be noticed, together with the reduced grid burden for district demand coverage. Correspondingly, this benefit also contributes to reducing the size of electric power transmission and conditioning devices, like power cables and transformers.

(4) For the H₂ station, the increased self-sufficiency rate of HVs results in the reduced H₂ transmission through the local pipelines. Such a feature helps to reduce the H₂ transmission cost of the H₂ station. For example, in the optimized Case 3 with the lowest powers of the electrolyzer and PEMFCs at 80 kW and 65 kW, respectively, 10.1% (3751.3 kg) of the annual total dispensed H₂ (36500 kg) for supporting regional transportation is produced by the onsite-renewable-electricity. Therefore, the H₂ delivered by the local pipelines is reduced which helps reducing the pipeline size and capital investment, and the corresponding transmission cost can be reduced by 10.1% within one year. Considering the H₂ transportation cost in California is 0.1-10.0 \$/kg [54], the annual H₂ transportation cost can be reduced by \$375.1-37513.0. Moreover, the increased renewable penetration ratio of the H₂ station through the peer-to-peer energy

sharing between adjacent buildings also contributes to reducing the CO₂ emission of H₂ infrastructure, which is beneficial for H₂ application in regional energy networks.

Table 5. Benefits for multiple stakeholders in the H₂-based district energy community with a H₂ station.

Assessment criteria	Level ^b					Practical benefits
	Reference case	Case 1	Case 2	Case 3	Case 3 ^c	
Houses						
Energy self-sufficiency rate	22.9%	24.0% (+1.1%)	28.4% (+5.5%)	40.6% (17.7%)	37.4% (+14.5%)	Improved energy independence
Annual total energy cost (\$/house)	2009.4	2009.4 (0)	1042.9 (-48.1%)	1329.2 (-33.9%)	1228.5 (-38.9%)	Reduced energy cost of every household
HVs						
Energy self-sufficiency rate	0	0 (0)	98.4% (+98.4%)	99.0% (+99.0%)	98.5% (+98.5%)	Less H ₂ transmission cost of H ₂ station
Renewable penetration rate	33%	33% (0)	98.9% (+65.9%)	99.3% (+66.3%)	99.0% (+66.0%)	Less CO ₂ emission of daily transportation
Annual H ₂ cost (\$/vehicle)	2096.1	2096.1 (0)	34.0 (-98.4%)	20.6 (-99.0%)	31.6 (-98.5%)	Reduced daily transportation cost
Local grid						
Max grid-import power ^a (kW)						
(1) Non-space-heating period	86.5	86.5 (0)	83.1 (-3.9%)	50.7 (-41.4%)	61.0 (-29.5%)	Reduced sizes of grid devices
(2) Space-heating period	103.2	103.2 (0)	103.2 (0)	103.2 (0)	78.2 (-24.2%)	
Max grid-export power ^a (kW)						
(1) Non-space-heating period	144.0	144.0 (0)	50.8 (-64.7%)	15.0 (-89.6%)	34.1 (-76.3%)	
(2) Space-heating period	103.0	103.0 (0)	26.1 (-74.7%)	4.8 (-95.3%)	18.1 (-82.4%)	
H₂ station						
Renewable penetration rate	33%	33%	39.9% (+6.9%)	43.0% (+10.0%)	41.8% (+8.8%)	Less CO ₂ emission of H ₂ infrastructure

^a: Mean hourly power.

^b: Real values with changes (compared to those of the reference case) in brackets.

^c: The minimum output power of V2G is 80 kW, and the minimum input power of the electrolyzer is 65 kW.

5 Discussion

Distributed renewable systems integrated with H₂ energy infrastructure provide a potential promising option for enhancing regional energy flexibility, power reliability, operational robustness, and system sustainability. A community-level regional energy system integrating electrical, thermal, and H₂ interactions, has been proposed, including low-rise

single houses, rooftop PV systems, HVs, a H₂ station with an electrolyzer, local power grid, and local H₂ pipelines. Unlike the impractical assumption of casual charging or discharging on electrolyzer and vehicle PEMFC systems in the academia (whenever there is surplus renewable or demand shortage), this study provides advances with considerations into the idling operating modes of the electrolyzer and vehicle PEMFCs as well as the two-stage cooling systems of PEMFCs, to guarantee both components to operate with high efficiency. Techno-economic benefits and system flexibility for multiple stakeholders have been quantitatively and comparatively analyzed from the perspectives of house owners, vehicle owners, local electric companies, and H₂ energy companies. The findings of this study have potential applications as follows:

(1) The advanced energy management strategies for integrating buildings, vehicles, H₂ station, local power grid and local H₂ pipelines, provide promising beneficial solutions for actualizing the zero-energy buildings-vehicles at a community level. To be specific, these strategies indicate how a residential community can make the best use of renewable energy, and meanwhile actualize significant peak-shaving and valley-filling effects on the local grid. These strategies also provide references for further developing current regional building energy-saving projects, such as the EcoBlock Project [49].

(2) For the current H₂ infrastructure development, such as the California Fuel Cell Revolution [55], H₂ stations are only designed for meeting transportation energy demands. The proposed energy strategies shed some light on the extension of H₂ station applications from only supporting regional transportation to powering regional buildings, supplying hot water, and releasing the power pressure on the local electric grid. The extended functions of H₂ stations can provide various energy support to regional building and transportation sectors as well as power supply infrastructure, which can undoubtedly promote the development of H₂ infrastructure in the regional energy network.

(3) In the district energy community herein, multiple stakeholders, including house owners, vehicle owners, local grid companies, and H₂ station companies, actively participate in the integration of buildings, HVs, grid, and H₂ station. The proposed energy management strategies illustrate promising techno-economic and environmental benefits for all participated stakeholders, which can be regard as the best motivation for these stakeholders to tightly collaborate on actualizing regional carbon neutralization. The parametric analysis in Section 4.3 also can provide references for further balancing multi-stakeholders' benefits by setting optimal critical parameters.

Furthermore, the limitations of this study are clarified to promote further studies:

(1) The proposed community only includes single type of houses with assumed deterministic schedules. Nonetheless, a practical community might include various building types, such as departments, supermarkets, and even offices, with different spatiotemporal characteristics of energy demands from single houses. Besides, due to the current pandemic around the whole world, people's life styles are changing and buildings might have longer occupied schedules with increased energy demands which might change the performance of current regional energy networks. Therefore, communities with various building types and different schedules need to be investigated in future studies.

(2) Now the renewable-produced H₂ price is set at 2-5 \$/kg [56], but California has no compensation policy for residential communities exporting surplus renewables to H₂ stations for H₂ production. This study uses the net H₂ consumption for calculating the H₂ cost. Such a simplification underestimates the H₂ cost because the onsite electrolyzers' maintenance cost and compressors' maintenance cost are not considered. Moreover, the hot water produced by cooling the electrolyzer in the H₂ station herein is free of cost to merge in the community's domestic hot water, which results in an underestimated cost of domestic hot water for the house owners.

(3) Although the heat recovery of the electrolyzer and PEMFCs is applied for providing domestic hot water, advanced heat recovery methods with heat pumps or absorption chillers can further improve heat recovery benefits to meet multiple building energy demands, such as space heating and space cooling. However, the integration of advanced heat

recovery methods needs more investigation.

(4) In the studied community, the surplus renewable electricity is only stored in the form of H₂ gas at the H₂ station. However, the electricity-H₂-electricity energy transfer procedure has a low efficiency at 40-50%, which elevates the whole system's energy loss. A possible solution is to adopt synergistic multiple energy storages to meet different energy demands at high efficiencies, such as electrochemical batteries for electricity storage and water tanks for thermal storage. A comprehensive analysis of the effects of synergistic energy storages on the H₂-station-integrated community is needed and will be investigated in our future studies.

(5) Combined application of electrochemical battery storage and H₂ storage to decelerate the battery cycling aging is a promising topic, in accordance with the intrinsic battery depreciation characteristics. Depending on the dynamic depth-of-discharging and number of cycles, different cycling aging rates of the battery can be noticed [43]. Depending on the idling power of electrolyzer and vehicle PEMFC, the flexible transition on smart charging/discharging between battery and H₂ systems will be studied to protect the battery relative capacity, enhance the renewable penetration and reduce the grid reliance.

(6) For now, HVs and PV panels are still expensive for low-income communities. Low-income people in California can cover their PV installation through participating in the Single-Family Affordable Solar Homes program or the Multi-family Affordable Solar Homes program [41], and then participate in the proposed energy network. However, for low-income people in other regions without the high subsidy for distributed renewable systems, more cost-efficient strategies and policies should be explored to promote people to participate in regional energy networks.

(7) The proposed energy network is assumed to be located near San Francisco with moderate climates, where natural ventilation is sufficient to maintain comfortable temperatures in summer. But in cases with the increasing atmosphere temperature caused by global warming or in other regions with extreme climates, space cooling is needed and the performance of the proposed energy network should be further explored.

6 Conclusions

This study proposes a solar-powered electricity-H₂ regional district energy system with thermal, electrical, and gas energy interactions for a community application, consisting of low-rise single houses, rooftop PV systems, HVs, a H₂ station with an electrolyzer, local power grid, and local H₂ pipelines, together with synergistic operations and electrical/thermal/H₂ interactions. Advanced power-to-gas conversion with chemical storages is applied to enhance the power supply reliability and grid stability, in response to intermittent renewable power generation. Four energy management strategies are proposed to improve techno-economic performance and system energy flexibility, focusing on the micro-grid for peer-to-peer energy sharing in building districts (Case 1), the H₂ station for renewable-to-H₂ conversion and storage (Case 2), the HVs to community micro-grid (V2G) interaction (Case 3). Moreover, a parametric optimization on the minimum powers of V2G interaction and electrolyzer is conducted to smartly control the charging/discharging of the H₂ system and balance seasonal grid stability and energy cost. The main findings of this study are listed as follows:

(1) The integration of the micro-grid community and H₂ station with V2G interaction (Case 3) outperforms other cases in terms of energy self-sufficiency and renewable penetration. As compared to the reference case (with the self-sufficiency rates at 22.9% and for 0 buildings and HVs, respectively), Case 3 elevates the energy self-sufficiency rates of the community buildings and HVs to 40.6% and 99.0%, respectively. Compared to the reference case (with the renewable penetration rates both at 33% for the H₂ station and HVs), Case 3 also increases the renewable penetration rates of the H₂ station and HVs to 43.0% and 99.3%, respectively.

(2) In terms of grid stability, among the four cases, the integration of the community and H₂ station with V2G interaction in Case 3 is the best solution for reducing the grid burden. Compared to the reference case, during the non-space-heating and space-heating periods, Case 3 reduces the maximum mean hourly grid-export power by and 89.6%

(from 149.5 to 15.0 kW) and 95.3% (from 103.0 to 4.8 kW), respectively. Case 3 reduces the maximum mean hourly grid-import power by 41.4%, from 86.5 to 50.7 kW, during the non-space heating period.

(3) In terms of annual energy consumption, due to a large amount of renewable electricity released into the H₂ system, the integration of the community and H₂ station (Cases 2 and 3) has relatively low annual net H₂ consumption at 2.1 and 1.2 kg/vehicle, respectively, much lower than the reference case and Case 1 at 127.0 kg/vehicle. However, Cases 2 and 3 show relatively high annual net grid electricity consumptions at 3457.1 and 4656.5 kWh/household, respectively, much higher than the isolated community and H₂ station in the reference case and Case 1 at -2888.8 kWh/household.

(4) In terms of annual energy cost, Case 2 with the integration of the community and H₂ station but without V2G interaction is the most cost-efficient strategy. To be specific, compared to the reference case (2009.4 \$/household), Case 1 does not reduce the electricity cost. Since much renewable electricity is released into the H₂ system in Cases 2 and 3, the electricity costs of Cases 2 and 3 rise up to 1008.9 and 1308.7 \$/household, respectively, but the annual H₂ costs are reduced to 34.0 and 20.6 \$/vehicle, respectively, with the costs of daily transportation at merely 0.002 and 0.001 \$/km, respectively. As a result, compared to the reference case, the total annual energy costs of Cases 2 and 3 are reduced by 48.1 and 33.9% for each household, respectively.

(5) Furthermore, elevating the minimum power of V2G interaction helps actualize seasonal energy storage and grid stability, and elevating the minimum input power of the electrolyzer reduces the energy cost of the community. The energy system of Case 3 with the minimum input power of the electrolyzer at 65 kW and the minimum power of V2G interaction at 80 kW can be regarded as a good balance for the annual grid stability and energy cost. Compared to the reference case, the energy planning and management in Case 3 can reduce the maximum mean hourly grid power to 78.2 kW (by 24.2%), and the annual energy cost to 1228.5 \$/household (by 38.9%).

Acknowledgments

This study is supported by the funding of Center for the Built Environment, University of California, Berkeley (Number: 59297 24003 44). This research is also supported by Hunan University, University of California and Lawrence Berkeley National Lab. All copyright licenses of have been successfully applied for all cited graphics, images, tables and/or figures.

References

- [1] European Environmental Agency. Final energy consumption by sector and fuel in Europe. <https://www.eea.europa.eu/data-and-maps/indicators/final-energy-consumption-by-sector-10/assessment> (2020).
- [2] U.S. Energy Information Administration. U.S. energy facts explained. <https://www.eia.gov/energyexplained/us-energy-facts/> (2020).
- [3] He Y, Li N, Lu J, Li N, Deng Q, Tan C, et al. Meeting thermal needs of occupants in shared space with an adjustable thermostat and local heating in winter: An experimental study. *Energy Build.* 2021;236:110776.
- [4] He Y, Li N, Zhang H, Han Y, Lu J, Zhou L. Air-conditioning use behaviors when elevated air movement is available. *Energy Build.* 2020;110370.
- [5] Zhou Y, Cao S, Kosonen R, Hamdy M. Multi-objective optimisation of an interactive buildings-vehicles energy sharing network with high energy flexibility using the Pareto archive NSGA-II algorithm. *Energy Conversion and Management.* 2020;218:113017.
- [6] Kafetzis A, Ziogou C, Panopoulos KD, Papadopoulou S, Seferlis P, Voutetakis S. Energy management strategies based on hybrid automata for islanded microgrids with renewable sources, batteries and hydrogen. *Renewable and Sustainable Energy Reviews.* 2020;134:110118.
- [7] Szima S, Nazir SM, Cloete S, Amini S, Fogarasi S, Cormos A-M, et al. Gas switching reforming for flexible power and hydrogen production to balance variable renewables. *Renewable and Sustainable Energy Reviews.* 2019;110:207-19.
- [8] Zhou Y, Cao S, Hensen JL, Lund PD. Energy integration and interaction between buildings and vehicles: A state-of-the-art review. *Renewable and Sustainable Energy Reviews.* 2019;114:109337.
- [9] Zhou Y, Cao S. Energy flexibility investigation of advanced grid-responsive energy control strategies with the static battery and electric vehicles: A case study of a high-rise office building in Hong Kong. *Energy Conversion and Management.* 2019;199:111888.

- [10] Abdin Z, Zafaranloo A, Rafiee A, Mérida W, Lipiński W, Khalilpour KR. Hydrogen as an energy vector. *Renewable and Sustainable Energy Reviews*. 2020;120:109620.
- [11] Toyota Motor Corporation. Toyota Ushers in the Future with Launch of 'Mirai' Fuel Cell Sedan. www.toyota-global.com/innovation/environmental_technology/fuelcell_vehicle/
- [12] Honda Motor Co. 2020 Honda CLARITY Fuel Cell. <https://automobiles.honda.com/clarity-fuel-cell> (2020).
- [13] Fuel Cell Promotion Office of Japan Agency for Natural Resources and Energy. About Fuel cell automatic vehicles. https://www.meti.go.jp/committee/kenkyukai/energy/suiso_nenryodenchi/suiso_nenryodenchi_wg/pdf/003_02_00.pdf (2014).
- [14] Mehrjerdi H, Bornapour M, Hemmati R, Ghiasi SMS. Unified energy management and load control in building equipped with wind-solar-battery incorporating electric and hydrogen vehicles under both connected to the grid and islanding modes. *Energy*. 2019;168:919-30.
- [15] Robledo CB, Oldenbroek V, Abbruzzese F, van Wijk AJ. Integrating a hydrogen fuel cell electric vehicle with vehicle-to-grid technology, photovoltaic power and a residential building. *Applied Energy*. 2018;215:615-29.
- [16] Farahani SS, Bleeker C, van Wijk A, Lukszo Z. Hydrogen-based integrated energy and mobility system for a real-life office environment. *Applied Energy*. 2020;264:114695.
- [17] Cao S, Alanne K. Technical feasibility of a hybrid on-site H₂ and renewable energy system for a zero-energy building with a H₂ vehicle. *Applied Energy*. 2015;158:568-83.
- [18] Felgenhauer MF, Pellow MA, Benson SM, Hamacher T. Evaluating co-benefits of battery and fuel cell vehicles in a community in California. *Energy*. 2016;114:360-8.
- [19] Sahu AV, Lee EHP, Lukszo Z. Exploring the potential of the vehicle-to-grid service in a sustainable smart city. 2018 IEEE 15th International Conference on Networking, Sensing and Control (ICNSC): IEEE; 2018. p. 1-6.
- [20] Alavi F, Lee EP, van de Wouw N, De Schutter B, Lukszo Z. Fuel cell cars in a microgrid for synergies between hydrogen and electricity networks. *Applied Energy*. 2017;192:296-304.
- [21] Oldenbroek V, Verhoef LA, Van Wijk AJ. Fuel cell electric vehicle as a power plant: Fully renewable integrated transport and energy system design and analysis for smart city areas. *International Journal of Hydrogen Energy*. 2017;42:8166-96.
- [22] Oldenbroek V, Wijtzes S, van Wijk A, Blok K. Fuel cell electric vehicle to grid & H₂: Balancing national electricity, heating & transport systems a scenario analysis for Germany in the year 2050. 2017 IEEE Green Energy and Smart Systems Conference (IGESSC): IEEE; 2017. p. 1-6.
- [23] Fuel Cell & Hydrogen Energy Association. Road Map to a US Hydrogen Economy <http://www.fchea.org/us-hydrogen-study> (2020).
- [24] California Energy Commission. Tracking Progress of Renewable Energy. https://www.energy.ca.gov/sites/default/files/2019-12/renewable_ada.pdf (2020).
- [25] U.S. Energy Information Administration. California Energy Consumption by End-Use Sector, 2018. <https://www.eia.gov/state/?sid=CA#tabs-2> (2020).
- [26] U.S. Energy Information Administration. Monthly Energy Review. https://www.eia.gov/totalenergy/data/monthly/pdf/sec10_3.pdf (2021).
- [27] California Fuel Cell Partnership. FCEV Sales, FCEB, & Hydrogen Station Data. https://cafcp.org/by_the_numbers (2020).
- [28] California Fuel Cell Partnership. The California Fuel Cell Revolution (CaFCP). <https://cafcp.org/sites/default/files/CAFRCR.pdf> (2018).
- [29] Toyota Company. 2021 MIRAI. <https://www.toyota.com/mirai/> (2021).
- [30] Alternative Fuels Data Center, U.S. Department of Energy. Hydrogen Laws and Incentives in California. <https://afdc.energy.gov/fuels/laws/HY?state=CA>
- [31] International Organization for Standardization. ISO 19880-1:2019 Gaseous hydrogen - Fueling stations - Part1: General requirements. 2019.
- [32] Qian F, Gao W, Yang Y, Yu D. Economic optimization and potential analysis of fuel cell vehicle-to-grid (FCV2G) system with large-scale buildings. *Energy Conversion and Management*. 2020;205:112463.
- [33] Zhou W, Yang L, Cai Y, Ying T. Dynamic programming for new energy vehicles based on their work modes Part II: Fuel cell electric vehicles. *Journal of Power Sources*. 2018;407:92-104.
- [34] Golden Gate Weather Services. CLIMATE OF SAN FRANCISCO. <https://ggweather.com/sf/narrative.html>.
- [35] ASHRAE Standard. Standard 90.2-2018 "Energy-Efficient Design of Low-Rise Residential Buildings". American Society of Heating, Refrigerating and Air-Conditioning Engineers, Inc Atlanta, GA, USA. 2018.
- [36] ASHRAE Standard. Standard 62.2-2019 "Ventilation for Acceptable Indoor Air Quality in Low-Rise Residential Buildings". American Society of Heating, Refrigerating and Air-Conditioning Engineers, Inc Atlanta, GA, USA. 2019.
- [37] CA 2007 Plumbing Code, Chapter 4. https://inspectapedia.com/plumbing/California_Plumbing_Code_Ch04.pdf (2000).
- [38] Parker DS, Fairey PW, Lutz JD. Estimating daily domestic hot-water use in North American homes. *ASHRAE Trans*. 2015;121.
- [39] NeON® R ACe Solar Panels. [https://www.lg.com/us/business/download/resources/CT00002151/LG370-380A1C-V5_PRE_FinalVer_083019\[20190921_023718\].pdf](https://www.lg.com/us/business/download/resources/CT00002151/LG370-380A1C-V5_PRE_FinalVer_083019[20190921_023718].pdf)
- [40] LG NEON R ACE LG375A1C-V5 375W MONO SOLAR PANEL W/ LG MICRO. <https://www.solaris-shop.com/>
<https://doi.org/10.1016/j.enconman.2021.114834>
<https://escholarship.org/uc/item/61g3g267>

- [lg-neon-r-ace-lg375a1c-v5-375w-mono-solar-panel-w-lg-micro/](#) (2021).
- [41] Sendy A. What solar incentives and rebates are available to California homeowners in 2021? <https://www.solarreviews.com/blog/california-solar-incentives-calculator> (2021).
- [42] NEWSROOM TU. Toyota fuel cell vehicle demonstration program expands. http://pressroom.toyota.com/article_display.cfm?article_id=1840 (2010).
- [43] Kurtz J, Sprik S, Bradley TH. Review of transportation hydrogen infrastructure performance and reliability. *International Journal of Hydrogen Energy*. 2019;44:12010-23.
- [44] Partnership CFC. Hydrogen Station Map. <https://cafcp.org/stationmap> (2020).
- [45] Partnership CFC. Cost to refill. <https://cafcp.org/content/cost-refill> (2020).
- [46] Company PG&E. ELECTRIC SCHEDULE E-TOU-D. https://www.pge.com/tariffs/assets/pdf/tariffbook/ELEC_SCHEDS_E-TOU-D.pdf (2020).
- [47] Company PG&E. Understand Net Energy Metering and your bill. https://www.pge.com/en_US/residential/solar-and-vehicles/green-energy-incentives/solar-and-renewable-metering-and-billing/net-energy-metering-program-tracking/understand-net-energy-metering.page (2020).
- [48] Company PG&E. Getting credit for surplus energy. https://www.pge.com/en_US/residential/solar-and-vehicles/green-energy-incentives/getting-credit-for-surplus-energy/getting-credit-for-surplus-energy.page (2020).
- [49] EcoBlock - California Institute for Energy and Environment, UC Berkeley. <https://ecoblock.berkeley.edu/> (2020).
- [50] A TRANSIENT SYSTEMS Simulation Program. Mechanical Engineering Department, UW Madison. <https://sel.me.wisc.edu/trnsys/> (2017).
- [51] Míguez J, López-González L, Sala J, Porteiro J, Granada E, Morán J, et al. Review of compliance with EU-2010 targets on renewable energy in Galicia (Spain). *Renewable and Sustainable Energy Reviews*. 2006;10:225-47.
- [52] Zhou Y, Cao S. Coordinated multi-criteria framework for cycling aging-based battery storage management strategies for positive building–vehicle system with renewable depreciation: Life-cycle based techno-economic feasibility study. *Energy Conversion and Management*. 2020;226:113473.
- [53] Zhou Y, Cao S, Hensen JL, Hasan A. Heuristic battery-protective strategy for energy management of an interactive renewables–buildings–vehicles energy sharing network with high energy flexibility. *Energy Conversion and Management*. 2020;214:112891.
- [54] U.S. Department of Energy. Costs of Storing and Transporting Hydrogen. <https://www.energy.gov/eere/fuelcells/downloads/costs-storing-and-transporting-hydrogen> (2014).
- [55] California Fuel Cell Partnership. A California Fuel Cell Revolution: A vision for 2030. <https://cafcp.org/blog/california-fuel-cell-revolution-vision-2030> (2019).
- [56] International Renewable Energy Agency. Making Green Hydrogen a Cost-Competitive Climate Solution. <https://www.irena.org/newsroom/pressreleases/2020/Dec/Making-Green-Hydrogen-a-Cost-Competitive-Climate-Solution> (2020).